Nano Research
2020, 13(10): 2579–2594
ISSN 1998-0124 CN 11-5974/O4
https://doi.org/10.1007/s12274-020-2722-z

Review Article

Nanomaterials for radiotherapeutics-based multimodal synergistic cancer therapy

Xi Yang[1], Ling Gao[1], Qing Guo[2], Yongjiang Li[1], Yue Ma[3], Ju Yang[3], Changyang Gong[1] (✉), and Cheng Yi[1] (✉)

[1] *Department of Medical Oncology, Cancer Center, West China Hospital, Sichuan University, Chengdu 610041, China*
[2] *Department of Oncology, Taizhou People's Hospital, Taizhou 225300, China*
[3] *Department of Pathophysiology, West China School of Basic Medical Sciences and Forensic Medicine, Sichuan University, Chengdu 610041, China*

Received: 23 December 2019 / **Revised:** 16 February 2020 / **Accepted:** 17 February 2020

ABSTRACT

Over the past decade, numerous studies have attempted to enhance the effectiveness of radiotherapy (external beam radiotherapy and internal radioisotope therapy) for cancer treatment. However, the low radiation absorption coefficient and radiation resistance of tumors remain major critical challenges for radiotherapy in the clinic. With the development of nanomedicine, nanomaterials in combination with radiotherapy offer the possibility to improve the efficiency of radiotherapy in tumors. Nanomaterials act not only as radiosensitizers to enhance radiation energy, but also as nanocarriers to deliver therapeutic units in combating radiation resistance. In this review, we discuss opportunities for a synergistic cancer therapy by combining radiotherapy based on nanomaterials designed for chemotherapy, photodynamic therapy, photothermal therapy, gas therapy, genetic therapy, and immunotherapy. We highlight how nanomaterials can be utilized to amplify antitumor radiation responses and describe cooperative enhancement interactions among these synergistic therapies. Moreover, the potential challenges and future prospects of radio-based nanomedicine to maximize their synergistic efficiency for cancer treatment are identified.

KEYWORDS

cancer treatment, radiotherapy, synergistic therapies, nanomaterials

1 Introduction

Cancer is one of the greatest challenges in worldwide healthcare. In the United States alone, 1,762,450 new cancer cases and 606,880 cancer deaths have been reported to date in 2019 [1]. Radiation therapy (radiotherapy, RT), involving external beam radiotherapy (EBRT) and internal radioisotope therapy (RIT), is a cornerstone of cancer treatment together with surgery and chemotherapy [2, 3]. RT has been used to eliminate cancer cells and overcome the recurrence of cancers. For EBRT, high-energy ionizing radiation (e.g., X-rays, proton or electron beams) delivered from outside the body has the capacity to induce cancer cell death with no depth restriction. As a result, EBRT either alone or in combination with other treatments is used extensively in the clinic for the treatment of local solid tumors involving brain, head and neck, breast, lung, colorectal, esophageal, liver, and prostate cancers [3–8]. For RIT, therapeutic radioisotopes are introduced into the tumor using minimally invasive procedures through brachytherapy, or via tumor targeting carriers administered intravenously [9, 10]. RIT has been developed for treatment of local tumors as well as bone metastases of malignancy [11–13]. However, RT remains limited for cancer treatment as a result of many apparently insurmountable shortcomings. First, because of the low radiation energy absorption coefficient of soft tissue tumors, high-dose radiation is often required to eliminate cancer cells efficiently, resulting in unavoidable collateral damage to adjacent normal tissues [14]. In addition, due to the presence of cancer stem cells and different cancer subtypes, some types of cancers are often highly resistant to RT [15]. Moreover, RT efficacy can be decreased by the hypoxic environment inside the tumor [15, 16]. Consequently, strategies to reduce radiation-induced side-effects and the development of radiosensitizers as well as *in vivo* targeted delivery of radioisotopes have attracted considerable attention in the field of RT [15, 17].

The rapid development of nanomaterials can play an important role in combating these challenges to improve cancer RT. Recently, nanomaterials for RT enhancement have been shown to act not only as radiosensitizers, but also as carriers for the delivery of therapeutic units [17–19]. On the one hand, due to Compton scattering, nanomaterials containing with high Z elements, including Au, Pt, Ba, and Bi, have high mass energy absorption coefficients for X-rays, which exacerbates radiation damage to the tumor and reduces the side-effects toward surrounding normal tissues [20, 21]. On the other hand, nanocarriers can be loaded with a large number of therapeutic units for delivery to tumors though active targeting and passive targeting by the enhanced permeability and retention effect (EPR) [22–24]. Therapeutic units include antitumor drugs, photosensitizers, photothermal agents, gas, genes, immune checkpoint inhibitors, immunotherapy adjuvant, and therapeutic radioisotopes [25–30].

Address correspondence to Changyang Gong, Chygong14@163.com; Cheng Yi, yicheng6834@126.com

Numerous nanomaterials have been developed to provide the strategies for improving RT. Nevertheless, despite the appreciable progress achieved in enhancing RT, the use of this technology in isolation has limited efficacy to eliminate cancer cells. As a result, current research on nanomaterials for the radio-based cancer therapy is shifting from RT monotherapy to radio-based multimodal therapies to improve RT efficacy and reduce side-effects [17]. The preparation and applications of nanomedicine for enhancing cancer RT have been discussed in previous reviews [18, 19, 21, 31]. Here, we focus mainly on nanomaterials for multimodal synergistic cancer therapies combining EBRT or RIT with other treatment modalities, including chemotherapy, photodynamic therapy (PDT), photothermal therapy (PTT), gas therapy, genetic therapy, immunotherapy, and trimodal synergistic therapies (Fig. 1). Moreover, we describe the technical challenges and key issues for the radio-based synergistic cancer therapy in the field of nanomedicine, with the intention of advancing its clinical translation.

2 Nanomaterials for EBRT-chemotherapy of cancers

The combination of EBRT and chemotherapy has emerged as a standard cancer treatment and achieved optimum and synergetic effectiveness for the treatment of various solid tumors [32]. This advantage is due to the ability of EBRT to improve local tumor control combined with the ability of chemotherapy to inhibit systemic metastatic tumors [33, 34]. Moreover, compared to EBRT alone, radio-chemotherapy hinders the sublethal damage repair and the intrinsic or acquired radiation resistance [35]. However, concurrent radio-chemotherapy is significantly more toxic than either the single mode treatments alone or sequential treatments [36].

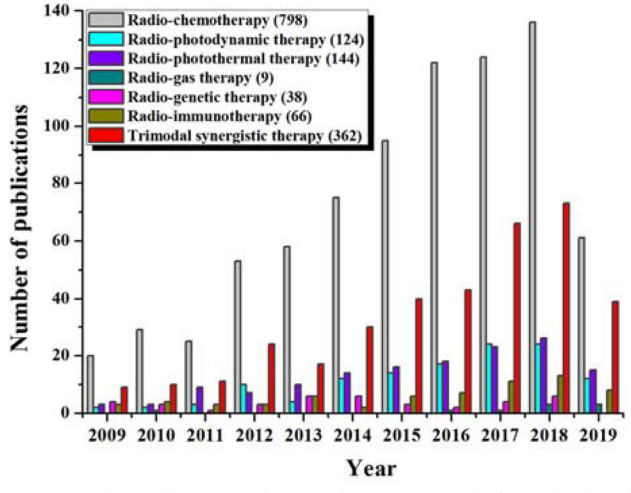

Figure 1 The publications about each nanomaterials for radio-based multimodal synergistic cancer therapy in the past decades. We used PubMed, and the search terms were "nanomaterials" + "radiotherapy" + "chemotherapy", "nanomaterials" + "radiotherapy" + "photodynamic therapy", "nanomaterials" + "radiotherapy" + "photothermal therapy", "nanomaterials" + "radiotherapy" + "gas therapy", "nanomaterials" + "radiotherapy" + "genetic therapy", "nanomaterials" + "radiotherapy" + "immunotherapy", and trimodal synergistic therapies ("nanomaterials" + "radiotherapy" + "chemotherapy" + "photodynamic therapy" or "photothermal therapy", or + "gas therapy", or + "genetic therapy" or + "immunotherapy"; "nanomaterials" + "radiotherapy" + "photodynamic therapy" or "photothermal therapy", or + "gas therapy", or + "genetic therapy", or + "immunotherapy"; "nanomaterials" + "radiotherapy" + "photothermal therapy", or + "gas therapy", or + "genetic therapy" or + "immunotherapy"; "nanomaterials" + "radiotherapy" + "gas therapy", or + "genetic therapy" or + "immunotherapy"; "nanomaterials" + "radiotherapy" + "genetic therapy" + "immunotherapy"), respectively.

Therefore, to promote the therapeutic efficacy and reduce the systemic toxicity of EBRT-chemotherapy, a promising strategy to incorporate nanomaterials into EBRT-chemotherapy is urgently required for clinical cancer treatment (Table 1) [37, 38].

2.1 Organic nanoparticles

2.1.1 Liposomes

Liposomes have both a hydrophobic and a hydrophilic region, allowing the encapsulation and delivery of both insoluble and soluble chemotherapy drugs [39]. Notably, liposomes are a versatile drug carrier that can be used to enhance the accumulation of chemotherapy drugs in the tumor while decreasing the concentration in normal tissues [40]. This characteristic of liposomes elevates the therapeutic efficacy and lowers the toxicity compared to that of the free chemotherapy drugs. Thus, the cooperation of EBRT and liposomal chemotherapy drug may enhance synergy between EBRT and chemotherapy.

As an example of this, Davies and co-workers developed liposomal doxorubicin (Caelyx) combined with additional single or fractionated RT for human osteosarcoma xenografts [41]. Both chemo-irradiation regimens achieved significant tumor growth delays compared with the two treatments administered separately. In terms of the mechanism underlying the enhanced antitumor effect, the results revealed that RT improved intratumoral doxorubicin uptake and distribution by a factor two to four. Cisplatin (CDDP) is a highly effective antitumor agent and can improve radiosensitization via the Compton scattering effect or the induction of cell cycle arrest, although the renal toxicity is unsatisfactory. Zhang et al. studied a new cancer treatment strategy involving sequential delivery of CDDP using nanoliposomes (NLE-CDDP), which can enhance the CDDP concentration in tumors and decrease its renal toxicity [42]. In this context, NLE-CDDP was shown to suppress A549 cell growth *in vitro*, and its toxicity was 2.35 times that found for free CDDP. Moreover, *in vivo* experiments of the treatment in a Lewis lung carcinoma model revealed the strongest radiosensitization in the 72 h interval between NLE-CDDP and irradiation.

The major limitation of radio-chemotherapy is the oxygen deficiency or hypoxia in the tumor environment. Radio-chemotherapy has insufficient capacity to eliminate tumor cells in hypoxic areas, resulting in the failure of this treatment for some solid tumors. Recently, safe and efficient hypoxic radiosensitizers have been used to enhance cancer radio-chemotherapy. Liu et al. prepared a hypoxic radiosensitizer-prodrug liposome (MLP) based on cholesterol, 1, 2-distearoyl-sn-glycero-3-phosphoethanol amine-N-methoxy-poly (ethylene glycol 2000) (DSPE-PEG2000), and hypoxic radiosensitizer nitroimidazoles conjugated with lipid molecules (MDH) for the delivery of doxorubicin (DOX) in the treatment of malignant glioma [43]. *In vivo* bioluminescence imaging studies indicated that MLP/DOX has the ability to penetrate the blood-brain barrier and deliver DOX into glioma tumors owing to the EPR effect. Moreover, MLP/DOX conjugated with 2-methyl-5-nitroimidazole-1-ethanol (MI)-grafted MDH lipid molecules has the ability to improve radiosensitivity and induce rapid release of DOX under hypoxic conditions, leading to synergetic radio-chemotherapy against glioma.

Hypoxic relief of tumors is another strategy for improving the effects of radio-chemotherapy. The antioxidant enzyme catalase (Cat) converts endogenous hydrogen peroxide (H_2O_2) into H_2O and O_2 inside the tumor, which is expected to increase the tumor reoxygenation. For instance, Zhang and co-workers

Table 1 Selected examples of nanomaterials for EBRT-chemotherapy of cancers[a]

Nanomaterials	Nanocarriers	Drug	Cancer type	Radiation dose (*in vivo*)	Biological effect		Ref.
					In vitro	*In vivo*	
Liposomes	Caelyx	Doxorubicin	Human osteosarcoma	8 Gy or 3.6 Gy daily×4	—	Induced significant tumor growth delays and worked synergistically	[41]
	NLE-CDDP	Cisplatin	Lewis lung carcinoma	2 Gy, 6 Gy, 16 Gy or 28 Gy	NLE-CDDP toxicity was 2.35 times that observed in CDDP	NLE-CDDP resulted in a higher therapeutic gain factor than did CDDP (4.28 vs. 2.70)	[42]
	MLP	Doxorubicin	Glioma	2 Gy daily×3	Enhanced the cellular uptake and promoted the release of DOX inside hypoxic glioma cells	Inhibited glioma growth	[43]
	CAT@Pt(IV)-liposome	Catalase and cisplatin (IV)	Breast cancer	6 Gy	Induced the highest level of DNA damage in cancer cells after X-ray radiation	Offered the most effective inhibition effect on tumor growth	[44]
Micelles	DLN	Paclitaxel	Glioblastoma multiforme	3 Gy daily×4	Reduced the *in vitro* viability of tumor cells	Suppressed brain tumor growth and prolonged survival	[46]
	MPEG-PCL/PTX polymeric micelles	Paclitaxel	Human cervical carcinoma	3 Gy daily×5	—	Suppressed tumor cell proliferation and inhibited angiogenesis	[47]
	HA-Fe-Nis-DOX	Doxorubicin	Prostate cancer	3 Gy	Induced strong radiosensitizing effects on hypoxic tumor cells	Lead to significant inhibition of tumor growth	[48]
Other organic nanoparticles	DOC-NPs	Docetaxel	Gastric cancer	5 Gy daily×3	Enhanced G2/M arrest, increased ROS, more effective DSBs and promoted apoptosis	Enhanced radiotherapeutics efficacy	[49]
	Albumin-bound paclitaxel	Paclitaxel	Ovarian adenocarcinoma or mammary carcinoma	10 Gy or 2 Gy daily×5	—	Exhibited strong antitumor efficacy	[50]
Inorganic nanoparticles	Cetuximab-IONPs	Cetuximab	Glioblastoma	10 Gy or 10 Gy daily×2	Observed antitumor effect	Increased in overall survival	[51]
	MnO_2-functioned ANPs-PTX	Paclitaxel	Colon cancer	5 Gy	Enhanced radiotherapy efficiency	Overcame the hypoxic microenvironment and enhanced the effect of chemoradiation therapy	[52]
	FA-GSJNs-DOX	Doxorubicin	Hepatocellular carcinoma	5 Gy	Induced synergistic anticancer effects	Exhibited remarked inhibition of tumor growth	[53]
	SeC@MSNs-Tf/TAT	Selenoamino acid	Cervical cancer	2 Gy	Induced radiosentization effect and enhanced radiation-induced apoptosis	Inhibited tumor growth	[54]
	mTa_2O_5-PEG/DOX	Doxorubicin	Breast cancer	6 Gy	Evidenced the excellent radiosensitizing ability	Improved therapeutic efficacy and reduced systemic toxicity	[55]

[a]Notes: Caelyx, liposomal doxorubicin; NLE-CDDP, nanoliposome encapsulated cisplatin; MLP, hypoxic radiosensitizer-prodrug liposome; MPEG-PCL/PTX polymeric micelles, methoxy poly(ethylene glycol)-poly(ε-caprolactone)/paclitaxel polymeric micelles; DLN, drug-loaded nanocarrier; HA-Fe-NIs-DOX, hyaluronic acid-amphiphilic ferrocenium-hexane-nitroimidazole-doxorubicin; Cetuximab-IONPs, magnetic iron-oxide nanoparticles bioconjugated to cetuximab; MnO_2-functioned ANPs-PTX, manganese dioxide-functioned albumin bound paclitaxel nanoparticles; FA-GSJNs-DOX, folic acid-Au-mesoporous silica Janus-doxorubicin-NPs; SeC@MSNs-Tf/TAT, selenoamino acid@multifunctional mesoporous silica nanoparticles-transferrin/TAT cell penetrating peptide; mTa_2O_5-PEG/DOX, mesoporous tantalum oxide-polyethylene golycol/doxorubicin; —, this is no mention in this paper.

encapsulated Cat inside liposomes to form Cat@Pt(IV)-liposomes containing the cisplatin (IV) pro-drug-conjugated DSPE (Pt(IV)-DSPE), cholesterol, PEG-conjugated DSPE, and 1, 2-dipalmitoyl-snglycero-3-phosphocholine (DPPC) [44] Cat@Pt(IV)-liposomes were found to retain and protect Cat activity to generate additional oxygen and reduce hypoxia. The concurrent delivery of Cat@Pt(IV)-liposomes and X-ray radiation resulted in the highest level of DNA damage in breast cancer cells under hypoxic conditions compared with that in the control groups. As shown in Fig. 2, *in vivo* studies of this form of combined radio-chemotherapy indicated that Cat@Pt(IV)-liposome mediated a superb synergistic suppression of tumor growth.

2.1.2 *Micelles*

Micelles are another type of hydrophobic/hydrophilic nano-structures that have been employed as a drug delivery system, especially to improve the bioavailability of insoluble chemotherapy drugs. Several different types of micelles have been shown to enhance the therapeutic efficacy and reduce the systemic toxicities of radio-chemotherapy [45]. In one study, drug-loaded nanocarriers (DLNs) consisting of filomicelles with novel hydrophilic-linked-hydrophobic block copolymers of poly (ethylene oxide)-block-poly (ε-caprolactone-random-D, L-lactide)

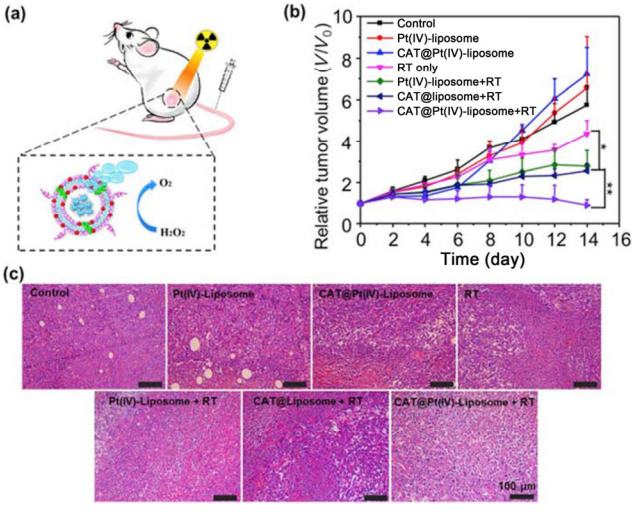

Figure 2 *In vivo* chemo-radiotherapy cancer therapy. (a) A scheme showing combined chemo-radiotherapy with CAT@Pt(IV)-liposome. (b) Tumor growth curves of mice after various different treatment indicated. V and V_0 stand for the tumor volumes after and before the treatment, respectively. Error bars were based on five mice in each group. All mice received twice injections of indicated materials at day 1 and day 2 and then were exposed to X-ray radiation at 24 h p.i. Day 0 refers to the day that the first dose X-ray radiation was applied. The doses of Pt and catalase were 3.3 and 2 mg/kg, respectively, the dose of X-ray was 6 Gy. (c) Micrographs of H&E-staining of tumor slices collected from mice of different groups at day 4. The combined chemo-radiotherapy with CAT@Pt(IV)-liposome resulted in the most significant damages to tumor cells. P values were calculated by the Student's t-test: $^*P < 0.1$, $^{**}P < 0.01$ ($n = 5$). Reproduced with permission from Ref. [44], © Elsevier 2017.

(OCLA), could be used to incorporate paclitaxel for the treatment of glioblastoma multiform (GBM) [46]. *In vivo* studies showed that paclitaxel-loaded nanocarriers combined with cranial RT markedly suppressed tumor growth compared with the control groups, and prolonged survival time by > 50%, due to the improvement of DLNs delivery to the intracranial tumor. In addition, methoxy poly (ethylene glycol)-poly (ε-caprolactone) (MPEG-PCL) polymeric micelles were designed to encapsulate hydrophobic drugs, forming a stable water-based formulation with lower toxicity for potential cancer treatment. Yu et al. reported that paclitaxel encapsulated in MPEG-PCL polymeric micelles (MPEG-PCL/PTX) synergized with RT in the treatment of human cervical carcinoma [47]. *In vivo* results displayed the higher antitumor effect of MPEG-PCL/PTX polymer micelles than that of PTX when combined with RT.

To further enhance the synergetic effects of radio-chemotherapy for tumors, Mao et al. designed self-assembly HA-Fe-NIs-DOX micelles based on DOX, ferrocenium (Fe, antitumor effect), and nitroimidazoles (NIs, hypoxic cell radiosensitizers), modified with hyaluronic acid through electrostatic interactions [48]. Due to the properties of NIs and Fe under hypoxia conditions and a high level of glutathione (GSH) in the tumor environment, HA-Fe-NIs-DOX micelles provoked rapid release of DOX inside prostate tumor cells. It was found that radio-chemotherapy with HA-Fe-NIs-DOX micelles showed highly selective radiosensitizing effects on hypoxic tumor cells, and induced the highest antitumor effect compared with the use of chemotherapy or RT alone.

2.1.3 *Other organic nanoparticles*

Some types of organic polymeric nanoparticles have also been developed as drug carriers for synergetic radio-chemotherapy against tumors. Cui et al. reported novel docetaxel-loaded nanoparticles (DOC-NPs) including a gelatinase-cleavage peptide with a PEG- and PCL-based structure for radiosensitizer DOC delivery in three gelatinase-overexpressing gastric cancers [49]. It was found that the highly selective radiosensitizing efficacy of DOC-NPs resulted in increasing reactive oxygen species (ROS) levels and enhancing apoptosis induction and cell cycle arrest in the G2/M phase. Owing to the gelatinase-stimuli targeting strategy, DOC-NPs act as radiosensitizers in gastric tumors while sparing normal tissues. In addition, 130 nm albumin-bound paclitaxel (nab-paclitaxel, Abraxane) nanoparticles were designed to enhance antitumor efficacy and reduce normal tissue toxicity [50]. *In vivo* results showed that when used in combination, nab-paclitaxel and RT enhanced RT efficacy by decreasing the dose of radiation yielding 50% tumor control from 54.3 Gy to 35.2 Gy. Thus, nab-paclitaxel plus RT exhibited stronger antitumor efficacy and lower toxicity than that of the control group for ovarian or mammary carcinomas.

2.2 Inorganic nanoparticles

The additional advantages of inorganic nanoparticles over their organic counterparts depend on their capability to act as a theranostic agent or efficient radiosensitizer. Some inorganic nanoparticles, such as manganese dioxide (MnO_2), gold, mesoporous silica, tantalum (Ta), and iron oxide have been verified to boost the antitumor efficiency of radio-chemotherapy [19, 51]. The albumin-bound paclitaxel nanoparticles (ANPs-PTX) mentioned previously were licensed for use in radio-chemotherapy by the United States Food and Drug Administration (FDA) in 2005. Recently, to overcome tumor hypoxia and further improve radio-chemotherapy of colorectal cancer, Meng et al. synthesized MnO_2 coated ANPs-PTX (MANPs-PTX) by conjugating MnO_2 on the outside of ANPs-PTX via a simple oxidation method. It was found that the MnO_2 shell of MANPs-PTX could decompose the abundant H_2O_2 into oxygen in the tumor microenvironment with excess H_2O_2 and acidic pH for tumor oxygenation [52]. In addition, MANPs-PTX coated with Mn^{2+} had strong T_1 magnetic resonance (MR) performances for imaging-guided therapy. Importantly, compared with the control group, the combination of MANPs-PTX and RT treatment showed the most significant inhibition (96.57%) of tumor growth.

Gold nanoparticles (Au NPs) have been used as drug carriers in radio-chemotherapy due to their outstanding properties and high Z radiosensitization ability. In one study, to enhance radiation absorption efficiency and avoid surface area hindrance, Wang et al. fabricated Janus-structured gold-mesoporous silica nanoparticles (GSJNs) via a modified sol-gel method (Fig. 3) [53].

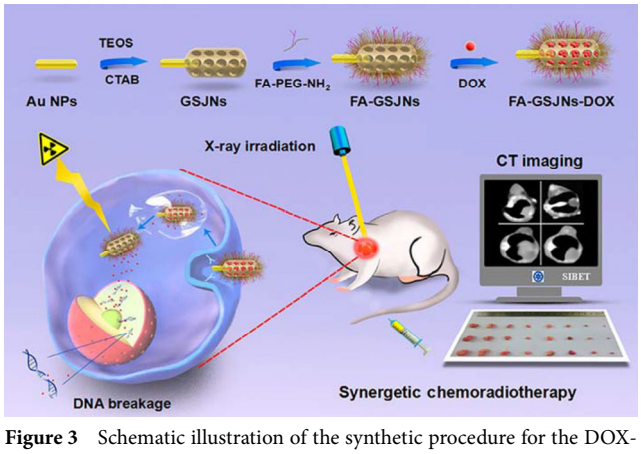

Figure 3 Schematic illustration of the synthetic procedure for the DOX-loaded Au-Mesoporous silica Janus NPs and application for synergetic chemoradiotherapy and CT imaging in HCC theranostics. Reproduced with permission from Ref. [53], © American Chemical Society 2017.

Subsequently, DOX was loaded in the GSJNs conjugating folic acid (FA) via a pH-sensitive linker. The resulting novel multifunctional theranostic FA-GSJNs-DOX facilitated effective hepatocellular carcinoma (HCC) targeting and pH-controlled DOX release. Thus, the theranostic FA-GSJNs-DOX offers the advantage of RT, chemotherapy, and computed tomography (CT) imaging into a multifunctional nanoplatforms. Notably, upon radiation, FA-GSJNs-DOX promoted antitumor effects *in vitro* and induced significant HCC growth suppression *in vivo* without any systemic toxicity.

Mesoporous silica nanoparticles (MSNs) serve as inorganic carriers for antitumor agents owing to low toxicity, high drug-encapsulating capability, and susceptibility to biological degradation. Interestingly, conjugation of transferrin protein (Tf) and TAT cell penetrating peptide to the surface of MSNs via a biodegradable poly (D, L-lactic-co-glycolic acid) (PLGA) linker to generate MSN-Tf/TAT promoted their internalization by cervical cancer cells though receptor-mediated endocytosis [54]. To further improve the sensitivity to RT, the efficient radiosensitizer selenocystine (SeC) was encapsulated in MSN-Tf/TAT to achieve synergistic radio-chemotherapy. Additionally, SeC@MSN-Tf/TAT improved cell growth suppression by X-ray exposure *in vitro* via generating oxidative stress and enhancing of ROS-mediated apoptosis. Furthermore, *in vivo* studies suggested that the combination of the dual-function SeC@MSN-Tf/TAT and RT remarkably delayed cervical tumor growth along with a marked reduction in damage. Based on the structure of MSNs that facilitates toxic radiosensitizer loading, Liu et al. prepared mesoporous tantalum oxide (mTa_2O_5) nanoparticles with PEG modification for enhanced radio-chemotherapy using a simple one-step soft template method [55]. Those mTa_2O_5-PEG nanoparticles were not only used as carriers for DOX, but also mediated highly selective sensitization to X-ray induced by RT. Radio-chemotherapy combined with mTa_2O_5-PEG/DOX nanoparticles showed significantly synergistic antitumor effects *in vivo* without any obvious systemic toxicities compared to free DOX.

2.3 Other delivery systems

As *in situ* drug delivery platforms, carrier hydrogels have been found to enhance anticancer drug concentrations in tumor tissues, facilitate controlled drug release, and subsequently reduce systemic toxicity. To avoid the high initial burst release in a diffusion-controlled hydrogel-based drug delivery system, liposome- or micelle-encapsulated drugs incorporated into the hydrogel matrix have provide an efficient strategy for combined radio-chemotherapy with improved antitumor efficacy. Recently, liposome-in-gel-paclitaxel (LG-PTX) systems have been developed to deliver the radiosensitizer PTX and increase the residence time of PTX at the tumor site [56]. This system was composed of PTX-loaded soya lecithin liposomes incorporated into a porous 0.1% (v/v) gellan hydrogel. The LG-PTX combined with focal radiation doses (3 Gy daily ×5) significantly reduced tumor volumes and prolonged survival in the treatment of an animal model of melanoma. In another example, Xu et al. investigated the radiosensitization effect of a gel-based dual drug delivery system (PDMP), which consisted of co-loaded mPEG-PCL/PTX and cisplatin (DDP) in the PEG-PCL-PEG (PECE) hydrogel for cervical cancer combination therapy [57]. It was found that the PDMP hydrogel combined with RT (12 Gy) inhibited tumor growth, extended survival time, increased the induction of apoptosis and the ratio of cells in the G2/M phase, and decreased the expression of CD133, aldehyde dehydrogenase (ALDH1) and CD31 in tumor tissues.

3 Nanomaterials for EBRT-PDT of cancers

PDT is a new alternative treatment approach for cancer management of various carcinomas. PDT utilizes nontoxic photosensitizers (PSs) that are converted by light at specific wavelength in the existence of O_2, inducing the production of cytotoxic ROS [58]. Importantly, *in situ* production of ROS, typically singlet oxygen ($^1O_2$), can eliminate tumor cells directly and/or damage tumor blood vascular, resulting in tissue ischemia. So far, however, PDT has provided unsatisfactory treatment efficacy for deep-located tumors due to the intrinsically shallow tissue penetration of light (< 1 cm). To overcome this limitation, X-ray was used as a potential excitation source to interrupt the shallow tissue penetration of PDT [59]. Based on this concept, a new X-ray-induced PDT (X-PDT) system was developed in which scintillation or persistent luminescence were attached to the PSs. Upon X-ray irradiation, scintillation luminescence emitted from the nanoparticles activates PSs to generate $^1O_2$, which not only functions as a simple PDT activator, but can also be a synchronous combination of RT and PDT for cancer treatment [60].

X-PDT integrate both the strengths of PDT and RT, which attracted marked interest for cancer treatment [59–79]. In 2006, Chen et al. first proposed that X-PDT overcome the shallow penetration of PDT [80]. In this study, scintillation luminescence nanoparticles attached to PSs (porphyrins, fullerenes, and TiO_2 semiconductor nanoparticles) were used to augment the cancer cell killing efficiency of X-rays. However, the conversion efficiency of the employed nanoscintillators is limited. Therefore, the use of X-PDT to optimize nanoscintillators with strong X-ray excited optical luminescence (XEOL) as X-ray transducers has become a current focus of researches in this field. Such nanoscintillator include rare-earth element-based nanoparticles (e.g., LaF_3:Tb, LaF_3:Ce, $SrAl_2O_4$:Eu, $LiLuF_4$:Ce, CeF_3:Gd^{3+}, Tb^{3+}, etc.), metal-based nanoparticles (e.g., ZnO, SiO_2, TiO_2, etc.), and metal-organic layers (e.g., Hf-DBB-Ru, $[Hf_6O_4(OH)_4(HCO_2)_6]$ SBUs, etc.) [60, 81, 82].

3.1 Rare-earth element-based nanoparticles

Zou et al. reported a novel strategy for photodynamic activation in which Ce^{3+}-doped lanthanum (III) fluoride (LaF:Ce^{3+}) luminescent nanoparticles designed via a wet chemistry method were used as intracellular light source in prostate cancer treatment [83]. Subsequently, LaF:Ce^{3+} luminescent nanoparticles were loaded into PLGA microspheres following the incorporation of protoporphyrin IX (PPIX). Importantly, LaF:Ce^{3+} luminescent nanoparticles and PPIX have an overlapping green emission with a peak at around 520 nm. Upon X-ray irradiation (90 kV), X-ray energy from LaF:Ce^{3+}/DMSO nanoparticles was transferred to PPIX and $^1O_2$ was produced for effective tumor cell killing. Studies on prostate cancer cells indicated that X-rays activated LaF:Ce^{3+}/DMSO/PPIX/PLGA microspheres to induce oxidative stress, DNA fragmentation and mitochondrial damage.

Xie et al. designed a novel X-PDT nanosystem (M-SAO@SiO_2) consisting of a core of $SrAl_2O_4$:Eu^{2+} nanoparticles (SAO:Eu, a scintillator) and a coating MSN encapsulating merocyanine 540 (MC540, PS) [84]. In this nanosystem, SAO acted a strong luminescent scintillator to transform X-ray photons to visible photons. Upon X-ray irradiation, the XEOL of SAO at approximately 520 nm activated MC540, leading to cytotoxic $^1O_2$ production, which increased the elimination of cancer cells deep within cancer tissue. *In vivo* therapy studies in U87MG tumor-bearing mice revealed significant tumor suppression

and efficient tumor shrinkage in the M-SAO@SiO_2 and X-ray group. In contrast, rapid tumor growth was detected in the control group. Furthermore, this synergy between M-SAO@SiO_2 and RT in X-PDT treatment led to effective tumor suppression in H1299-tumor-bearing mice, even when the tumor was covered with a 2-cm pork tissue block. Additionally, there was no obvious toxicity when M-SAO@SiO_2 was used in the absence of RT.

Recently, the synergistic use of RT + X-PDT has been developed for combined and imaging-guided treatment of deeply located tumors. Co-doping is known mainly for its pivotal role in enhancing the scintillation of several materials. Ahmad et al. designed CeF_3 NPs co-doped with Gd^{3+} and Tb^{3+} (CeF_3: Gd^{3+}, Tb^{3+}) to enrich scintillation in deep-located tumors therapy [85]. CeF_3: Gd^{3+}, Tb^{3+} scintillating NPs were encapsulated with mesoporous silica. The resulting capsules were also loaded with FDA-approved rose Bengal (RB) (CGTS-RB NPs), which generates cytotoxic $^1O_2$ under X-ray irradiation. Moreover, the presence of a high Z element (Gd, 64) facilitated the incorporation of real-time CT and MRI diagnostics with radiosensitized features without radiation toxicity and/or observable systemic side-effects. The *in vivo* results demonstrated efficient tumor inhibition with dual-modal imaging (CT and MRI) guided nonradioactive synergistic RT + X-PDT compared to the use of RT alone. Additionally, global untargeted metabolome analysis revealed blockade of amino acid supply chain pathways as mechanism underlying this efficient tumor suppression mediated by X-ray-induced, synergistic RT + X-PDT treatment. This technique may provide new applications in deep-seated tumors within the tissues.

Subsequently, Zhong et al. also developed the cerium (Ce)-doped $NaCeF_4$:Gd,Tb scintillating nanoparticle (ScNP or scintillator) with uniform rod-like morphology for X-ray excited RT and radiodynamic therapy (RDT) [86]. Under X-ray excitation, Ce ions served not only as sensitizers to enhance the fluorescence emission of terbium (Tb) ions for RT, but also as photocatalysts in the production of ROS for RDT (Fig. 4). Owing to the high Z elements of Ce, Gd, and Tb ions, $NaCeF_4$:Gd,Tb ScNPs enhanced the local radiation dose deposition with additional multi-modality CT and MR imaging abilities. *In vitro* and *in vivo* experiments have indicated that synchronous RT/RDT with ScNPs achieved remarkable suppression of tumor growth in both CT26 tumor and A549 tumors without systemic toxicity.

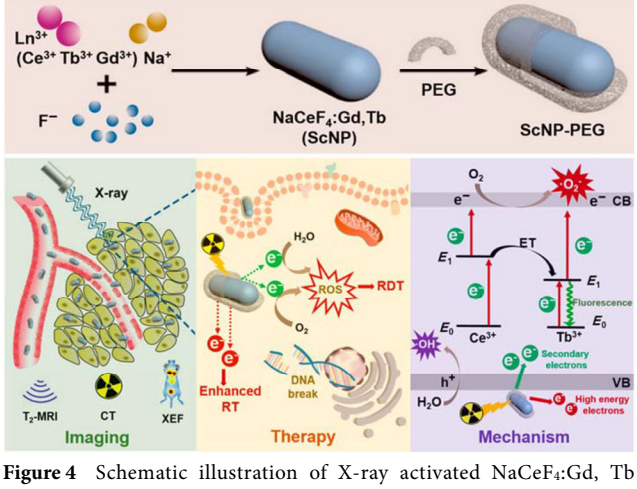

Figure 4 Schematic illustration of X-ray activated $NaCeF_4$:Gd, Tb scintillator for XEF/CT/T_2-MR imaging-guided synchronous RT and RDT of cancer. Reproduced with permission from Ref. [86], © American Chemical Society 2019.

3.2 Other metal-based nanoparticles

The application of other metal-based nanoparticles as radiosensitizers is a novel method of augmenting the treatment efficacy of low-dose X-PDT without systemic toxicity. For example, copper and cobalt co-doped ZnS (ZnS:Cu,Co) afterglow nanoparticles were prepared using a wet chemistry method and conjugated with the photosensitizer tetrabromorhodamine-123 (TBrRh123) [87]. Under X-ray excited luminescence, an efficient energy shift from ZnS:Cu,Co afterglow nanoparticles to TBrRh123 was detected. Because $^1O_2$ was produced for PDT activation, ZnS:Cu,Co-TBrRh123 conjugates were very effective for human prostate cancer treatment. Additionally, these afterglow nanoparticles were also utilized for cell imaging.

Recently, Chen and co-workers reported the development of photosensitizer-conjugated aggregation-induced emission heterogeneous Au clustoluminogens (AIE-Au) using glutathione-protected Au clusters (GCs) to obtain efficient X-PDT without systemic toxicity [88]. Following low-dose X-ray irradiation, AIE-Au strongly absorbed X-ray to induce hydroxyl radicals that enhance double-stranded DNA damage within tumors. In addition, the AIE-Au efficiently transformed X-rays to optical luminescence and activated the conjugated rose Bengal (RB), leading to a PDT effect via oxidizing lipid membranes. Moreover, anticancer studies in radioresistant cancer models, such as gastric carcinoma (U87MG), prostate cancer (PC3) and hepatocellular carcinoma (HepG2), indicated that R-AIE-Au treatment (1 Gy) induced more rapid tumor growth inhibition with minor toxicity than that observed in the RT group (5 Gy). The same group also designed a silicate nanoscintillator with uniform and controllable size by simply adjusting the high Z metal dopants to enhance the effects of X-PDT [89]. First, silicates with different XEOL were developed by the introduction of selective metal dopants (ZSM), such as Zn- and Mn-dopants. Second, the photosensitizer RB, which was conjugated to a silicate, which has the capacity to convert X-rays to PDT for X-ray imaging and RT. Third, the cyclic arginylglycylaspartic acid (RGD) peptide used for integrin-targeted tumor delivery was coupled with RB-ZSM to form RB-ZSM-RGD nanosensitizers. The synergistic functions of RB-ZSM-RGD, including XEOL, PDT, RT, and integrin-targeting were shown to enhance accumulation in tumors and improve tumor suppression under low-dose X-ray irradiation with reduced biological side-effects.

3.3 Metal-organic layers

In addition to rare-earth element-based nanoparticles and other metal-based nanoparticles, metal-organic layers (MOLs) have also be applied as X-ray converters. For instance, Li et al. designed a new class of tunable and functionalizable MOLs constructed from $[Hf_6O_4(OH)_4(HCO_2)_6]$ secondary building units (SBUs) and highly potent PSs of $Ir[bpy(ppy)_2]^+$ or $Ru(bpy)_3^{2+}$-derived tricarboxylate ligands to kill colon cancer cells [90]. As such, Hf atoms efficiently absorb X-ray and convert energy to $Ir[bpy(ppy)_2]^+$ or $Ru(bpy)_3^{2+}$ moieties for ROS production. *In vivo* experiments showed that Hf-MOLs induce excellent tumor inhibition in MC38 and CT26 cancer models, indicating the promise of Hf-MOLs for cancer treatment.

Mitochondria are essential for tumor cells proliferation, metastasis and invasion. From the early stage of PDT treatment, $^1O_2$ produced inside mitochondria efficiently damage mitochondria and augment the cytotoxic effects. To develop mitochondria-targeted PSs and maximize anticancer efficacy, the Li group synthesized a mitochondria-targeted nMOF, Hf-DBB-Ru [DBB-Ru=bis(2,2'-bipyridine) 5,5'-di(4-benzoato)-2,2'-bipyridine) ruthenium (II) chloride]. Elemental quantification and super-resolution confocal microscopy demonstrated that

Hf-DBB-Ru possessed a cationic UiO topology with a formula of $[Hf_6(\mu_3\text{-}O)_4(\mu_3\text{-}OH_4)(DBB\text{-}Ru)_6]$ by encapsulating $Ru(bpy)_3^{2+}$ into the framework, indicating a strong mitochondria-targeting property [91]. Hf-DBB-Ru-enabled RT-RDT generated hydroxyl radicals from the Hf_6 SBUs under low doses of highly penetrating X-rays, while $^1O_2$ was generated from the DBB-Ru PSs. This mitochondria-targeting RT-RDT process may, therefore, provide new possibilities for the release of cytochrome c, depolarization of the mitochondrial membrane potential, and disruption of the respiratory chain to initiate apoptotic pathways in cancer cells. Thus, this process will result in significant suppression of colorectal tumors at low X-ray doses without systemic toxicity.

4 Nanomaterials for EBRT-PTT of cancers

PTT has been developed rapidly for cancer management in the past few years owing to its favorable biosafety properties [92]. PTT commonly utilizes photothermal agents to induce heat under near-infrared (NIR) light irradiation to eliminate cancer cells in target tumor areas. Compared to traditional tumor treatment strategies (chemotherapy, surgery and RT), PTT has the advantages of high specificity, reduced side-effects, and minimal invasiveness in the ablation of cancer [93]. More importantly, the hyperthermia generated from PTT can improve tumor vascular perfusion, increase intratumoral blood flow, and enhance tumor oxygenation to overcome the tumor hypoxia. Nevertheless, the clinical application of PTT is hampered by its limited ability to kill deep-located cancer cells due to the depth-dependent laser intensity [94]. Therefore, EBRT combined with PTT can compensate for their individual drawbacks. The heat from PTT can enhance the oxygen content in tumors to increase their radiosensitivity, while EBRT can efficiently control deep-located tumors, leading to synergetic therapeutic effects [95]. Due to the dramatic improvement in nanomaterials, various NIR-dependent nanomaterials conjugated with photothermal agents, such as noble metal nanostructures, transition metal-based materials, carbon-based materials, and organic nanomaterials, have been widely used for PTT and EBRT synergetic therapy (Table 2).

4.1 Noble metal nanostructures

Recently, many noble metal plasmonic nanostructures, such as Au nanostructures, Pt-based nanocomposites, and Ir nanocrystals, have been used as both radiosensitizers and photothermal agents owing to their X-ray absorption properties and NIR absorption ability [93]. The potential of all these Au nanostructures with high atomic number (Z = 79) and surface

Table 2 Typical examples of nanomaterials for EBRT-PTT of cancers[a]

Photoabsorbers	Therapeutic agents	Photothermal materials	Radiosensitizers	X-ray dose (Gy)	Thermal effect (λ; power; t; T)	Imaged guided	Cell lines	*In vivo*	Ref.
Noble metal nanostructures	Fe_3O_4/Au DSNFs	Au	Au	4	808 nm; 1.2 W/cm^2; 5 min; ~ 55 °C	PA/CT/MR	4T1	*In vivo*	[96]
	MnO_2-mSiO_2@Au-HA nanoparticles	Au	Au	6	808 nm; 1.5 W/cm^2; 5 min; ~ 60 °C	MOST/CT/MR	4T1	*In vivo*	[97]
	PtRu-PEG BNCs	Ru/Pt	Pt	4	808 nm; 0.75 W/cm^2; 10 min; ~ 60 °C	CT	4T1	*In vivo*	[98]
	Ir@liposome	Ir nanocrystals	Ir	6	785 nm; 0.8 W/cm^2; 20 min; ~ 45 °C	PA	4T1	*In vivo*	[99]
	OPCNs-PEG-FA	OPCNs	Pt	10	808 nm; 2.4 W/cm^2; 5 min; ~ 53 °C	PA	HepG2	*In vivo*	[100]
	Ti_3C_2@Au nanocopsites	Au/Ti_3C_2	Au	6	1,064 nm; 0.75 W/cm^2; 10 min; ~ 52.5 °C	PA/CT	4T1	*In vivo*	[101]
Transition mental-based materials	WS_2-IO/S@MO-PEG nanocomposites	WS_2	W	4	808 nm; 0.5 W/cm^2; 10 min; —	PA/MR	4T1	*In vivo*	[102]
	WS_2 quantum dots	WS_2	W	6	808 nm; 1.0 W/cm^2; 10 min; ~ 45 °C	PA/CT	BEL-7402	*In vivo*	[103]
	PEGylated $Cu_3Bi_2S_3$ nanorods	Bi_2S_3	Bi	8	1,064 nm; 1 W/cm^2; 6 min; ~ 55 °C	PA/CT	4T1	*In vivo*	[104]
	MnSe@Bi_2Se_3-PEG nanostructures	Bi_2Se_3	Bi	4	808 nm; 0.6 W/cm^2; 20 min; ~ 45 °C	MR/CT	4T1	*In vivo*	[105]
	PVP-Bi_2Se_3@Sec NPs	Bi_2Se_3	Bi	6	808 nm; 1 W/cm^2; 10 min; ~ 57.2 °C	—	BEL-7402	*In vivo*	[106]
	MoS_2 quantum dots@polyaniline	MoS_2	Mo	6	808 nm; 1.5 W/cm^2; 5 min; ~ 54.8 °C	PA/CT	4T1	*In vivo*	[107]
	$NaYbF_4$:Er/Gd@SiO_2-NH_2-PEG-CuS nanoparticles	CuS	Yb, Er, Gd	6	980 nm; 1.5 W/cm^2; 5 min; ~ 52.5 °C	UCL/CT/MR	Hela	*In vivo*	[108]
Carbon-based materials	PVP-PG	rGO	Bi, W	6	808 nm; 0.35 W/cm^2; 10 min; ~ 45 °C	PA	Hela	*In vivo*	[109]
Organic nanomaterials	CCPA@PPy NGs	PPy	—	4	808 nm; 1.0 W/cm^2; 5 min; ~ 50 °C	PA	4T1	*In vivo*	[110]

[a]Note: Fe_3O_4/Au DSNFs, generation 5 (G5) poly (amidoamine) dendrimer-stabilized Au nanoflowers (Au DSNPs) and stabilized ultrasmal iron oxide (USIO/Fe_3O_4) nanoparticles; CT, computed tomography; MR, mganetic resonance; PA, photoacoustic; MSOT, multispectal optoacoustic tomography; OPCNs, concave PtCu octopod nanoframes; Pt, platinum; Ru, ruthenium; PtRu-PEG BNCs, multifoliate PEGylated PtRu bimetallic nanocomplexes; Ir, iridium; WS_2, tungsten disulfide; PVP-Bi_2Se_3@Sec NPs, poly (vinylpyrollidone)-and selennocysteine-modified Bi_2Se_3 nanoparticles; UCL, upconversion luminescence; PVP-PG, a bismuth heteropolytungstate-based radiocatalytic sensitizer; rGO, rediced grahene oxid; PPy, polypyrrole; CCPA@PPy NGs, polypyrrole-loaded γ-polyglutamic acid (γ-PGA) nanogels; —, this is no mention in this paper.

plasmon resonance (SPR) oscillations to serve as radiosensitizers as well as photothermal agents to enhance the EBRT and PTT efficiency have been explored. For instance, Lu et al. studied the formation of a unique multifunctional theranostic nanoplatform (Fe_3O_4/Au DSNFs) for a multimode T_1-weighted MR/CT/photoacoustic (PA) imagine-guided combination of PTT and RT in a murine breast tumor model. The Fe_3O_4/Au DSNFs were prepared via self-reduction and a hydrothermal method based on generation 5 (G5) poly (amidoamine) dendrimer-stabilized Au nanoflowers (Au DSNPs) and stabilized ultrasmall iron oxide (USIO/Fe_3O_4) nanoparticles [96]. Tumor growth was significantly suppressed by treatment with Fe_3O_4/Au DSNFs + laser + RT compared to that observed in other groups ($P < 0.05$). Moreover, the survival time of the mice were increased by 40 days after treatment with Fe_3O_4/Au DSNFs + laser + RT. For another example, Wang et al. synthesized innovative multifunctional nanotheranostic MnO_2-$mSiO_2$@Au-HA nanoparticles (MAHNPs) based on MnO_2-$mSiO_2$ nanohybrids (MNHs) and AuNPs via electrostatic adsorption for multispectral optoacoustic tomography (MSOT)/MR/CT triple modal imaging-guided hypoxia-maneuvered and oxygen self-sufficiency RT [97]. These well-designed nanoparticles reversed tumor hypoxia by decomposing endogenous H_2O_2 to generate O_2, and improve cellular uptake via HA-surface modified MnO_2-$mSiO_2$@Au nanoparticles. The MAHNPs generated remarkable PTT and RT synergism resulting in almost complete eradication of tumors without observable recurrence *in vivo*. Beyond Au nanostructures, other investigations of noble metal-based RT and PTT, including multifoliate PEGylated PtRu bimetallic nanocomplexes (PtRu-PEG BNCs), Ir@liposome, and concave PtCu octopod nanoframes (OPCNs-PEG-FA), have also provided excellent synergistic antitumor effects in solid tumors [98–101].

4.2 Transition metal-based materials

Transition metal-based materials, such as tungsten disulfide (WS_2), Bi_2S_3, Bi_2Se_3, MoS_2, and CuS, represent photothermal agents that have provided a new strategy in PTT owing to their absorbance in the NIR region and efficient heat generation abilities, which can be used for multimodal imaging and cancer treatment [102–108]. In addition, certain types of transition metal-based materials, including WS_2, Bi_2Se_3, and MoS_2, which contain high Z elements, have served as enhancers for PTT and RT in the treatment of cancer. Liu et al. introduced WS_2-IO/S@MO-PEG nanocomposites for combined PTT and oxygen-enhanced RT and pH-responsive MR imaging [102]. The WS_2-IO/S@MO-PEG nanocomposites were designed using high quality WS_2 nanoflakes, which absorbed with iron oxide nanoparticles (IONPs), coated with silica and then subsequently with MnO_2 functionalized with PEG on their surface. In comparison with monotherapies, the combined WS_2-IO/S@MO-PEG + PTT + RT treatment mediated excellent inhibition of 4T1 tumor growth, which was attributed to a remarkable synergistic effect of the WS_2-IO/S@MO-PEG-mediated radiophotothermal therapy. The same group has also successfully fabricated multifunctional MnSe@Bi_2Se_3-PEG core-shell nanostructures using a cation exchange method for synergistic thermoradiotherapy in 4T1 tumor-bearing mice [105]. In these MnSe@Bi_2Se_3-PEG nanostructures, the paramagnetic MnSe core offers contrast for both T_1- and T_2-weighted MR imaging, whereas the Bi_2Se_3 shell endows the nanostructure with excellent NIR absorption that enables PTT as well as absorption of ionizing radiation for CT imaging and increased RT. *In vivo* studies showed that the combination of RT and PTT triggered by MnSe@Bi_2Se_3-PEG synergistically enhanced the therapeutic effects owing to the enhanced oxygenation from the mild PTT that overcomes hypoxia-associated radioresistance. Moreover, similar enhanced synergistic anticancer effects of PTT and RT can be obtained with MoS_2 quantum dots@polyaniline (MoS_2@PANI) inorganic-organic nanohybrids [107]. This versatile nanohybrid can also be used for simultaneous dual-modal PA/CT imaging (Fig. 5).

4.3 Carbon-based materials

Recently, the NIR absorption ability of reduced graphene oxide (rGO), a carbon-based material, facilitates its use as a photothermal agent for generating mild heat to improve intratumoral blood flow and decrease hypoxia-associated RT resistance. Due to the poor dispensability and stability of rGO in physiological solution, Zhou et al. synthesized bismuth heteropolytungstate (BiP_5W_{30}) nanoclusters to couple with rGO by promoting electron-hole separation to generate a bismuth heteropolytungstate-based radiocatalytic sensitizer (PVP-PG) [109]. In addition to these NIR-triggered PTTs, PVP-PG with high Z elements, like W and Bi, enhance X-ray radiation dose deposition in tumor tissues. Importantly, radioactive PVP-PG depletes glutathione (GSH) by a "redox-reaction effect" and catalyze the decomposition of H_2O_2 to toxic HO· via a "radiocatalytic effect". *In vivo* studies showed that PVP-PG effectively suppressed the growth of HeLa tumors in mice

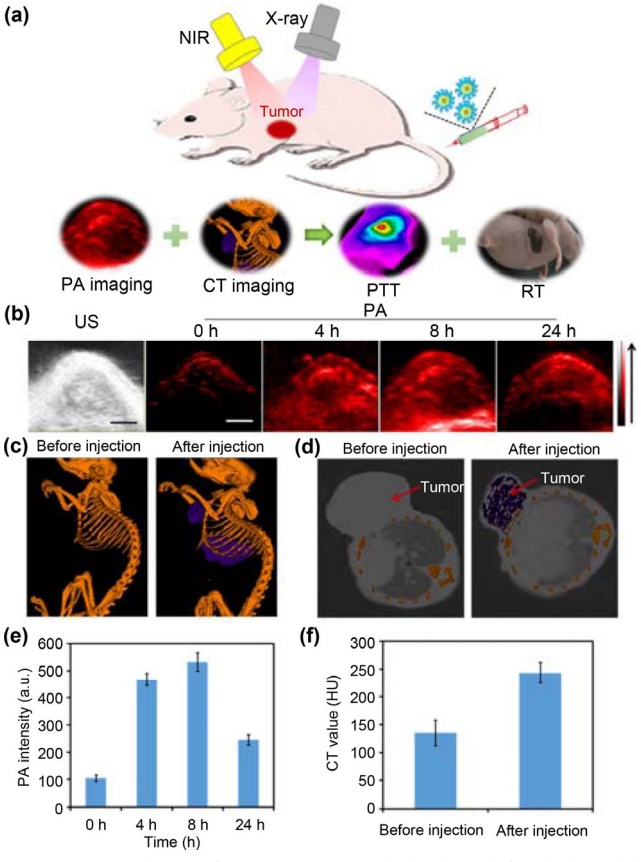

Figure 5 (a) Scheme of MoS_2@PANI nanohybrids used for dual modal imaging and combined PTT and RT therapy. (b) Ultrasound (US) images and PA images of 4T1 tumors after intraveously injected with MoS_2@PANI nanohybrids at different time points. (c) *In vivo* CT images of 4T1 tumor-bearing mice before and 8 h afterintravenous injection with MoS_2@PANI nanohybrids. (d) *In vivo* CT images of tumors on mice before and 8 h after intravenous injection with MoS_2@PANI nanohybrids. (e) Corresponding intensity of the photoacoustic signal of MoS_2@PANI nanohybrids in the tumor at the different time points. (f) Correspongding HU value of MoS_2@PANI nanohybrids in the tumor before injection and 8 h after injection. Reproduced with permission from Ref. [107], © American Chemical Society 2016.

after both 808 nm laser irradiation and X-ray irradiation, demonstrating the significant synergistic therapeutic effect in radio-photothermal therapy treatment.

4.4 Organic nanomaterials

Similar to the inorganic photothermal agents mentioned previously, several organic nanomaterials, including polypyrrole (PPy), polyaniline (PANI), polythiophene, and organic dyes, have also been widely utilized as PTT agents for cancer treatment. This could be attributed to biocompatibility, biodegradability, optical stability, good NIR absorption, and thermal conversion of organic nanomaterials with high efficiency. To enhance the therapeutic efficiency of PPy, Zhou and co-workers reported the use of the cystamine dihydrochloride (Cys)-crosslinked γ-polyglutamic acid (γ-PGA) nanogels (CCPA NGs) to encapsulate PPy for RT-sensitized PTT of 4T1 tumors under thermal/PA imaging [110]. In detail, CCPA NGs were obtained by a double emulsion strategy, and then used as a nanoreactor for charged pyrrole monomer loading via electrostatic interaction in the presence of Fe(III) ions. The resulting CCPA@PPy NGs displayed an average diameter of 38.9 ± 8.6 nm with good colloid stability and water-dispensability. Compared to use in the reverse sequence (RT + PTT), tumors in mice with treatment of CCPA NGs were mostly suppressed followed by the sequence of PTT + RT. This high efficiency PTT/RT combination strategy for breast cancer suggested that mild hyperthermia (approximately 50 °C) improved blood flow in tumor sites and enhanced tumor oxygenation, which could enhance RT-sensitivity.

5 Nanomaterials for EBRT-gas therapy of cancers

Gas therapy using gases, including nitric oxide (NO), oxygen (O_2), carbon monoxide (CO), and hydrogen sulfide (H_2S), is an emerging "green" therapeutic modality in the management of cancer [111]. However, due to the difficulties in controlling gases *in vivo*, the therapeutic application of gases remains major challenge in the clinic [111]. To improve gas therapies, numerous nanocarriers have been developed for the efficient gas delivery and controllable gas release in lesions [111–113]. Moreover, these nanocarriers act synergistically with EBRT to enhance therapeutic responses.

5.1 NO

Fan et al. devised a multifunctional stimuli-responsive nano-theranostic system (PEG-USMSs-SNO) by loading upconverting nanoparticles (UCNPs) with S-nitrosothiol (R-SNO)-grafted mesoporous silica for simultaneous upconversion luminescent (UCL) imaging and an intelligent X-ray-controlled NO release in hypoxic tumors [114]. The PEG-USMSs-SNO responded to X-ray irradiation for selectively cleaving the S–N bond of SNO group to control NO release, while high NO concentrations in tumors acted as an effective hypoxic radiosensitizer to enhance RT responses. In addition, UCNPs could be used to provide a visually monitor drug delivery by UCL imaging/PET/MRI. Additionally, *in vivo* experiment results suggested that tumors treated with PEG-USMSs-SNO + RT were significantly inhibited compared with the effects of other treatments, indicating the increased NO-sensitized RT efficacy against cancer. These results also showed that X-ray controlled NO release from PEG-USMSs-SNO could overcome limited penetration and endogenous differences. The on-demand synergistic radio-gas therapy was expected to be important in establishing X-ray targeted NO release for deep-seated tumors without any side-effects.

As a powerful oxidizing and nitrating agent, peroxynitrite ($ONOO^-$) could be used to modulate complex biological processes and kill tumor cells through the derived NO and superoxide ($O_2^{\cdot-}$). However, because of the short half-life and diffusion distance of NO and $O_2^{\cdot-}$, simultaneous efficient generation of $ONOO^-$ in the same region is required. To solve such problems, Du and co-workers developed a multifunctional X-ray targeted $ONOO^-$ generation platform with the UV–responsive NO donor Roussin's black salt (RBS) and scintillating nanoparticles (ScNPs, $LiLuF_4:Ce^{3+}$) for application in radiosensitization [115]. In this construct, Ce-doped $LiLuF_4$ not only served as a radiosensitizer for the generation of an abundance of ROS involving $O_2^{\cdot-}$ following X-ray irradiation, but also converted X-rays into UV light *in situ* to excite the surrounding RBS to generate NO. Following this, X-ray-excited concurrent release of NO and $O_2^{\cdot-}$ by ScNPs was shown to ensure the efficient generation of $ONOO^-$ in A549 cells. Synergistic X-ray targeted $ONOO^-$ and RT were shown to significantly inhibit the lung tumor growth due to the enhancement of DNA damage and suppression of PARP-associated DNA self-repair. Additionally, the released NO and $ONOO^-$ could overcome the hypoxia-associated radioresistance by serving as hypoxia inducible factor-1α (HIF-1α) inhibitors and powerful vasodilators. What's more, ScNPs could be used as a contrast agent in CT imaging in cancer diagnosis. Thus, the system developed by Du et al. may offer a potential synergistic RT/gas therapy combination approach to improve lung cancer treatment.

5.2 O_2

Perfluorocarbon (PFC), which has high oxygen solubility, has been developed as an O_2 shuttle to combat the hypoxic tumor microenvironment and improve the efficacy of EBRT. For instance, Liu et al. designed and synthesized an artificial nanoscale red blood cell mimic system (PFC@PLGA-RBCM nanoparticles) by encapsulating PFC within a PLGA polymer to deliver O_2 and subsequently coating the exterior with a red blood cell membrane (RBCM) to prolong the half-life in the blood circulation [116]. Due to the smaller size of the PFC@PLGA-RBCM nanoparticles relative to native RBCs, the nanoparticles are able to carry O_2 into solid tumor by leaking out from the tumor vasculature to relieve the hypoxic status of the whole tumor. In a subcutaneous 4T1-tumor model, intravenous delivery of PFC@PLGA-RBCM nanoparticles enhanced the tumor suppressing efficacy of RT without any systemic toxicity. In addition, the same group designed novel hollow tantalum oxide (TaOx)@Cat nanoparticles with the ability not only to effectively deposit radiation energy within the tumor to enhance radiation-associated DNA damage, but also to deliver Cat to decompose H_2O_2 into H_2O and O_2 and combat hypoxia-induced RT resistance [117]. As a result, tumor growth was significantly inhibited in breast tumor-bearing mice, showing a synergistic RT sensitization effect of TaOx@Cat nanoparticles.

5.3 CO

CO induces the apoptosis of cancer cells by inducing mitochondrial dysfunction. Nanocarriers encapsulating CO-releasing molecules have been used to control CO release with improved delivery and bioavailability in tumor tissue. To overcome hypoxia-associated EBRT resistance, Fan and co-workers synthesized a series of small thioether-hybridized hollow mesoporous organosilica nanoparticles (HMONs) for co-loading of tert-butyl hydroperoxide (TBHP) and iron pentacarbonyl ($Fe(CO)_5$) using an ammonia-assisted hot water etching method [112]. Following

X-ray irradiation, the activated sequential bond within TBHP was selectively cleaved to induce the production of toxic ·OH, which not only leaded to irreversible cancer cell death in RDT, but also attacked $Fe(CO)_5$ to generate CO molecules via the gas release process. Subsequent results demonstrated that the cascade of ·OH and CO molecules produced from the TBHP/$Fe(CO)_5$ co-loaded HMONs nanoparticles mediated remarkable destructive effects on both hypoxic and normoxic tumors, without reliance on oxygen.

6 Nanomaterials for EBRT-genetic therapy of cancers

Genetic therapy provides an alternative strategy for enhanced RT efficacy [118]. RT commonly causes preferential tumor DNA damage. By precisely targeting the response to this DNA damage or HIF-1α with genetic therapy, it is possible to achieve potent radiosensitization while decreasing the side-effects on normal tissues [119, 120]. With the development of non-viral genetic delivery systems, nanocarriers used in synergistic EBRT-genetic therapy have demonstrated promising properties, including the ability to target tumor cells, improve DNA stability, and enhance RT efficiency.

For example, heat shock protein-microRNA-nanoparticles (Hsp70-miRNA-NP) were used to enhance the therapeutic efficacy of RT [121]. Since membrane Hsp70 expression was upregulated by X-ray irradiation, membrane Hsp70-specific antibodies could act as a tumor-specific target. In this design, cmHsp70 monoclonal antibodies were coupled to human serum albumin (HSA) NP encapsulating survivin miRNA-expressing plasmids that enhanced apoptosis. This system showed enhanced cellular uptake in LN229 and U87MG glioblastoma cells and reduced survivin expression compared to non-conjugated NPs. Moreover, *in vitro* experiments indicated that Hsp70-miRNA-NP irradiated with a dose of 2 or 8 Gy improved caspase 3/7 activity and reduced clonogenic cell survival.

Owing to the rapid progression of tumor cells and distorted tumor blood vessels, various types of malignant solid tumors are subject to the effects of insufficient oxygen supply (hypoxia). Notably, the hypoxic areas in the tumor microenvironment induce greater RT resistance compared to the normoxic areas, resulting in hypoxia-associated radiation resistance. Radiosensitization nanomaterial systems represent a new approach for overcoming radioresistance, by relieving tumor hypoxia and enhancing RT responses. Yong group integrated Gd-containing poly-oxometalate-conjugated chitosan (GdW_{10}@CS nanosphere) as an external radiosensitizer and delivered HIF-1α siRNA as an internal sensitizer into a radiosensitization system to combat radioresistance (Fig. 6) [122]. On the one hand, under X-ray exposure, GdW_{10}@CS nanospheres with high Z metal elements depleted the intracellular glutathione (GSH) to produce high levels of ROS by synergistic W^{6+}-triggered GSH oxidation. On the other hand, HIF-1α siRNA was used to knockdown HIF-1α expression in hypoxic tumors, thereby simulating poly (ADP-ribose) polymerase-1 (PARP-1) degradation, increasing caspase-3 expression, and inhibiting the repair of double-stranded DNA breaks. Moreover, GdW_{10}@CS nanospheres containing tungsten and gadolinium atoms also served as a dual-modal MR and CT imaging contrast agents, for real-time monitoring and cancer diagnosis and treatment of BEL-7402 tumors. As a result, significant tumor growth inhibition and no recurrence was investigated in the $GdW_{10}@CS_{siRNA}$ + RT group without any side-effects, which indicated that GdW_{10}@CS nanospheres reinforce both the extrinsic and intrinsic radiosensitization effects of RT.

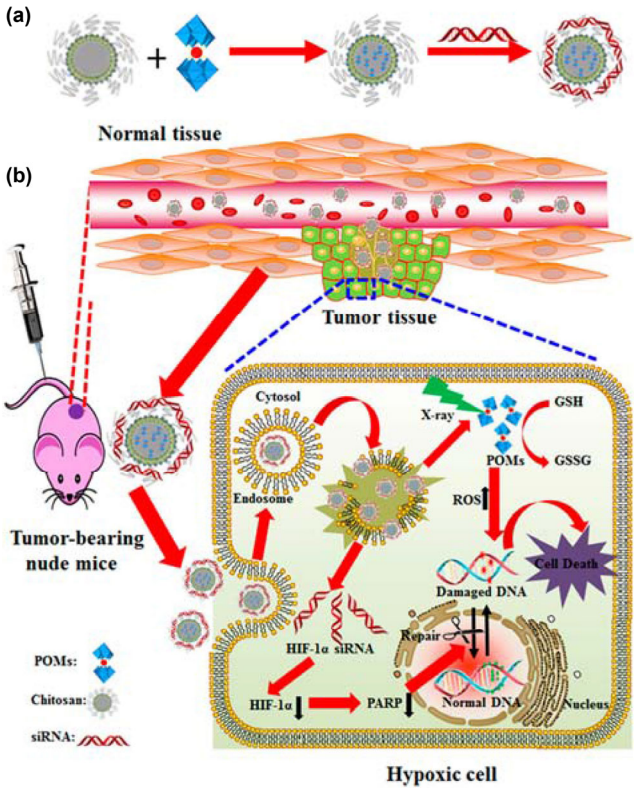

Figure 6 Schematic illustrations of the as-prepared Gdw_{10}@CS nanosphere as a siRNA delivery platform for efficient radiosensitization efficacy of radiotherapy against hypoxic tumor cells. Reproduced with permission from Ref. [122], © American Chemical Society 2017.

7 Nanomaterials for EBRT-immunology therapy of cancers

Cancer immunotherapy has emerged as a new method of management for patients with many types of cancer [123]. Cancer immunotherapies, such as checkpoint inhibitors and immune adjuvants, are designed to activate both antitumor immune cells in the tumor tissues and the host immune system to establish long-term immune memory [124]. Nonetheless, low patient responses rates and immune-related toxicities have limited their application in the clinic. Localized radiotherapy not only directly initiates cell death, but also induces immunogenic cell death as a form of *in situ* tumor vaccination that induces infiltration of macrophages, dendritic cells (DC), cytotoxic T cells, as well as suppressor cells, such as regulatory T (T_{reg}) cells, and myeloid-derived suppressor cells (MDSCs) [15, 125–130]. Therefore, radiotherapy not only enhances innate and adaptive antitumor immunity, but also exerts immunosuppressive responses. With the development of delivery systems, combination radiotherapy based on nanomaterials designed for immunotherapy offers opportunities to augment antitumor immunity and to decrease immunosuppression in a safe and effective manner [31].

In recent years, checkpoint inhibitors such as anti-CTLA4 (αCTLA4), anti-PD-1 (αPD-1), and anti-PD-L1 (αPD-L1) have shown powerful promise for improving the survival of patients with bladder cancer, non-small-cell lung cancers, melanoma, Hodgkin's lymphoma, and head and neck cancer [131]. However, response rates remain low at 10% to 20% [132]. Combining checkpoint inhibitors with RT has been demonstrated to not only augment local tumor control and but also elicit an "abscopal effect" by increasing the release of tumor-associated antigen and their cross presentation to enhance T cells priming

[129, 133, 134]. In a recent study, Min and co-workers reported that PLGA-based antigen-capturing nanoparticles (AC-NPs) with cancer functional groups captured tumor-derived protein antigens (TDPAs) that were delivered to antigen presenting cells and significantly enhanced αPD-1 responses after RT [135]. This group also found that the set of TDPAs captured by each AC-NPs was based on NP surface properties. Moreover, *in vivo* experiments showed that PLGA or Mal AC-NPs + RT + αPD-1 suppressed the growth of secondary tumors (unirradiated) and greatly increased the survival time compared to other treatments in a bilateral B16F10 melanoma model. Mechanistic studies of the abscopal effect indicated that PLGA and Mal AC-NPs under irradiation remarkably increased intratumoral $CD4^+T/T_{reg}$ and $CD8^+$ T/T_{reg} ratios.

In addition to checkpoint inhibitors, immune adjuvant is a key promoter of tumor immunotherapy. For example, unmethylated cytosine-guanosine dinucleotide (CpG) motifs, which act as a Toll-like receptor 9 (TLR9) agonist, are an attractive immunostimulatory agent that can be used to induce Type I interferons and proinflammatory cytokines via a MyD88/IRF7/NF-κB-dependent pathway [136]. However, the antitumor immunity induced by CpG is limited due to untargeted immunostimulation with a systemic cytokine storm. Recently, an amphiphilic form of CpG (amph-CpG) was designed to enhance tumor-specific delivery though conjugation of an albumin-binding analog of CpG. Because X-irradiation contributes to improve tumor microvascular permeability, this study showed that increased accumulation of amph-CpG in irradiated tumors corresponded with increased tumor control that was relative to either treatment alone, while off-target accumulation in kidneys and liver were reduced. Moreover, the combination of RT and amph-CpG treatment increase interferon gamma and granzyme B activity, and activated both intratumoral and circulatory $CD8^+$ T cells and monocytes/macrophages.

8 Nanomaterials for EBRT-based trimodal synergistic therapies of cancers

In addition to the EBRT-based bimodal synergistic therapy for cancer mentioned previously, trimodal synergistic therapies are based on cooperative incremental interactions between modalities including RT, chemotherapy, PDT, PTT, gas therapy, genetic therapy, and immunotherapy [137, 138]. For instance, Chen et al. synthesized core-shell nanoparticles (PLGA-R837@Cat nanoparticles) based on PLGA by loading Cat inside the aqueous cavity and loading imiquimod (R837) into the PLGA shell [139]. When these PLGA-R837@Cat nanoparticles accumulated into tumor tissues as a result of the EPR effect, Cat decomposed H_2O_2 to generate O_2, which overcame the tumor hypoxia. At the same time, R837 functions as an immune adjuvant to enhance a robust antitumor immune response. Mice treated with PLGA-R837@Cat nanoparticles under X-ray irradiation showed much higher *in vivo* antitumor efficacy than that of RT alone. Moreover, in a study of PLGA-R837@Cat nanoparticle-based RT combined with anti-CTLA4, the tumor-associated antigens from post-radiotherapy-induced immunogenic cell death not only suppressed tumor metastases through a very strong abscopal effect, but also prevented cancer recurrence via the production of effective long-term immunological memory. These findings suggested a synergetic cancer treatment of RT/gas therapy/immunotherapy.

To develop an effective theranostic nanoplatform, Guo et al. synthesized BiOI@Bi_2S_3@BSA semiconductor heterojunction nanoparticles (SHNPs) in a simple two-step process [140]. This platform was used for multimodal CT/photoacoustic (PA) imaging using triple-combination therapy: RT, PDT and PTT. On the one hand, SHNPs were found to possess superior radiosensitization owing to the presence of the high Z elements (I atoms and Bi). On the other hand, the SHNPs functioned as a semiconductor under the X-ray irradiation to induce ROS production based on electron-hole pairs for PDT, owing to the good photocatalytic properties of bismuth oxyiodide (BiOI). Additionally, because of the strong NIR photothermal conversion properties of Bi_2S_3, SHNPs were also found to have the ability to generate mild photothermal effects that increased the intratumoral blood flow and relieved the tumor hypoxia. Here, BLE-74 tumor formation in mice treated with SHNPs was significantly inhibited under X-ray irradiation, which suggesting that a synergistic antitumor efficacy of RT/PDT/PTT is superior to any of the individual treatments.

9 Nanomaterials for RIT-based synergistic therapy of cancers

In addition to the use of nanomaterials in EBRT-based tumor combination therapies to enhance antitumor efficiency, nanomaterials are also good options for therapeutic RIT-based synergistic therapies that improve RIT efficacy. RIT has been combined with other types of treatments, including chemotherapy, PTT, and gas therapy, using delivery system to simultaneously transfer radioisotopes and other therapeutic units into tumors to obtain synergistic effect [9, 17, 141].

9.1 RIT-chemotherapy

Recently, various types of micelles or nanoparticles have been designed for co-delivery of radioisotopes and drugs for combined RIT/chemotherapy. For example, Shih et al. designed multifunctional micelles (PEG-b-PCL) co-loaded with the radionuclide rhenium-188 (^{188}Re) and DOX to achieve synergetic RIT-chemotherapy for hepatocellular carcinoma [142]. Following delivery of the ^{188}Re-DOX micelles, tumor growth was inhibited and the survival was prolonged in the murine hepatocellular carcinoma model, which suggested that the synergistic RIT-chemotherapy was more effective than either of the individual modes alone. Werner et al. also developed a RIT-chemotherapy cancer treatment strategy by simultaneously delivering paclitaxel and yittrium-90 (^{90}Y) into tumors using folate-targeted nanoparticles [143]. *In vivo* studies showed that the combination of paclitaxel and yittrium-90 (^{90}Y) induced a significantly therapeutic effect on an ovarian cancer peritoneal metastasis model.

9.2 RIT-PTT

To enhance the synergistic anti-tumor effects, nanomaterial-modulated synergetic RIT-PTT was observed by co-delivery of the radioisotopes and photothermal agents using nanocarriers. For example, Zhou and co-workers designed a PEG-coated [^{64}Cu] copper sulfide (CuS) nanoparticle platform that incorporated the plasmonic properties of CuS nanoparticles and the radioactive properties of ^{64}Cu [144]. CuS converts the light energy obtained from NIR laser treatment into thermal energy for tumor thermal-ablation of human ATC cells Hth83. Moreover, ^{64}Cu delivers a high radiation dose and realizes positron emission tomography (PET) imaging. PEG[^{64}Cu]CuS nanoparticles significantly improved the survival of Hth83 tumors compared to either option alone and without acute toxic effects. In another study, Chen et al. integrated the radioisotope ^{131}I and the photothermal agent nano-graphene oxide (RGO) to form ^{131}I-RGO-PEG to obtain a combination of RIT and PTT against cancer [145]. The radio-ionization effect of ^{131}I induced

cancer killing, and the strong NIR absorbance of RGO enabled effective photothermal ablation of tumors. Treatment of animals bearing 4T1 breast cancer with ^{131}I-RGO-PEG under 808 nm laser exposure resulted in effective elimination of tumors.

Recently, Liu et al. reported a NIR-triggered hybrid hydrogel system using ^{131}I-labeled CuS (CuS/^{131}I) nanoparticles as radiotherapeutics, the photothermal agent, 2,2'-azobis[2-(2-imidazolin-2-yl) propane] dihydrochloride (AIPH) as the thermal initiator, and poly(ethylene glycol) double acrylates (PEGDA) as polymeric matrix for RIT/PTT synergistic treatment (Fig. 7) [146]. Due to the polymerization of PEGDA by exciting the AIPH thermal initiator, locally injected CuS/^{131}I-PEGDA/AIPH solution was rapidly transformed into a gel *in situ* following 915 nm NIR-induced photothermal heating. With CuS/^{131}I nanoparticles fixed in the tumors in this way, repeated NIR irradiation induced significant heat production and achieved prolonged relief of the tumor hypoxia and further improved the efficacy of the ^{131}I isotope. Thus, CuS/^{131}I nanoparticles in PEGDA gel enable the synergistic photothermal brachytherapy effect that destroys tumor cells in a "one injection, multiple treatments" strategy.

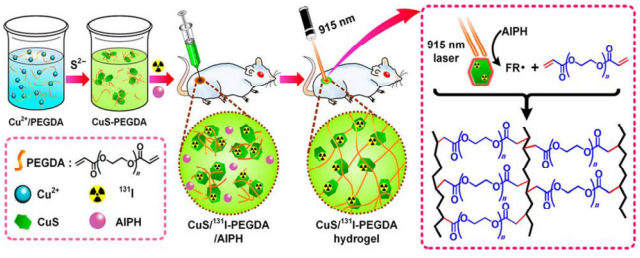

Figure 7 Scheme showing the controllable *in situ* synthesis of CuS/^{131}I-PEGDA hydrogel in the tumors of mice. Reproduced with permission from Ref. [146], © American Chemical Society 2018.

9.3 RIT-gas therapy

To overcome hypoxia-associated RIT resistance, Tian and co-workers developed radionuclide ^{131}I labeled HAS-bound MnO_2 (^{131}I-HAS-MnO_2) nanoparticles as a multifunctional RIT nanomedicine platform [147]. On the one hand, ^{131}I-HAS-MnO_2 nanoparticles exhibit highly efficient EPR-derived tumor retention for RIT and nuclear imaging. On the other hand, MnO_2 induces the production of O_2 from H_2O_2 under acidic conditions in the tumor, which relieves tumor hypoxia and enhances the efficacy of RIT. Furthermore, ^{131}I-HAS-MnO_2 nanoparticle treatment showed significant antitumor therapeutic effects in mice bearing 4T1 tumors, suggesting that a synergistic efficacy of RIT/gas therapy is superior to any of the individual options.

10 Conclusions and future perspectives

Here, we have comprehensively discussed the significant developments made in this promising field of nanomaterials that have improved RT efficacy. The summarized studies show that radio-based bimodal or trimodal synergistic therapies cooperatively enhance interactions between RT and other therapeutic modalities to improve the RT antitumor efficiency and reduce the common shortcomings associated with conventional therapies. Despite the advances in nanomaterials for radio-based tumor combination therapies, several key issues and challenges remain to be addressed to pave the way for future developments. First, the in-depth and sophisticated mechanisms of radio-based bimodal and trimodal synergistic therapies require further investigations to maximize their cooperative efficacy and reduce radiation-induced side-effects by using molecular and genetic technologies. Second, the long-term biosafety and tumor targeting efficiency of radio-based nanomedicines may play important roles in improving antitumor synergistic efficiency. Third, more efforts are need to optimize the multifunctional characteristics of nanomaterials for RT enhancement. Fourth, the radiation dose and fractionation schedule used in these combination therapies remain to be established. Finally, in addition to the therapeutic effects outlined here, more synergistic therapeutics may also be generated by combining RT with other therapeutic strategies to combat cancer, such as chemodynamic therapy, monoclonal antibody therapy, and starvation therapy.

In spite of several unresolved issues, nanomaterials for radio-based synergistic therapeutics are a potential research hotspot that warrants further exploration. Additionally, with the development of on-demand combination RT, radio-based nanomedicines offer significant promise for their clinical translation as cancer therapies.

Acknowledgements

This research was supported by the Post-Doctor Research Project, West China Hospital, Sichuan University (No. 2018HXBH032) and Sichuan Science and Technology Program (No. 2019YFS0109), 1.3.5 project for disciplines of excellence, West China Hospital, Sichuan University (No. ZYJC18035), China Postdoctoral Science Foundation (No. 2019M663505), and Postdoctoral Interdisciplinary Innovation Foundation, Sichuan University (No. 0040204153243).

References

[1] Siegel, R. L.; Miller, K. D.; Jemal, A. Cancer statistics, 2019. *Ca-Cancer J. Clin.* **2019**, *69*, 7–34.

[2] Chan, S.; Rowbottom, L.; McDonald, R.; Bjarnason, G. A.; Tsao, M.; Danjoux, C.; Barnes, E.; Popovic, M.; Lam, H.; DeAngelis, C. et al. Does the time of radiotherapy affect treatment outcomes? A review of the literature. *Clin. Oncol.* **2017**, *29*, 231–238.

[3] Schaue, D.; McBride, W. H. Opportunities and challenges of radiotherapy for treating cancer. *Nat. Rev. Clin. Oncol.* **2015**, *12*, 527–540.

[4] Corradini, S.; Krug, D.; Meattini, I.; Matuschek, C.; Bölke, E.; Francolini, G.; Baumann, R.; Figlia, V.; Pazos, M.; Tonetto, F. et al. Preoperative radiotherapy: A paradigm shift in the treatment of breast cancer? A review of literature. *Crit. Rev. Oncol. Hematol.* **2019**, *141*, 102–111.

[5] Lee, V. H.-F.; Yang, L.; Jiang, Y.; Kong, F.-M. S. Radiation therapy for thoracic malignancies. *Hematol. Oncol. Clin. N* **2020**, *34*, 109–125.

[6] Lu, L.; Li, W.; Chen, L.; Su, Q.; Wang, Y.; Guo, Z.; Lu, Y.; Liu, B.; Qin, S. Radiation-induced intestinal damage: Latest molecular and clinical developments. *Future Oncol.* **2019**, *15*, 4105–4118.

[7] Kalogeridi, M.-A.; Zygogianni, A.; Kyrgias, G.; Kouvaris, J.; Chatziioannou, S.; Kelekis, N.; Kouloulias, V. Role of radiotherapy in the management of hepatocellular carcinoma: A systematic review. *World J. Hepatol.* **2015**, *7*, 101–112.

[8] King, R. B.; McMahon, S. J.; Hyland, W. B.; Jain, S.; Butterworth, K. T.; Prise, K. M.; Hounsell, A. R.; McGarry, C. K. An overview of current practice in external beam radiation oncology with consideration to potential benefits and challenges for nanotechnology. *Cancer Nanotechnol.* **2017**, *8*, 3.

[9] Hamoudeh, M.; Kamleh, M. A.; Diab, R.; Fessi, H. Radionuclides delivery systems for nuclear imaging and radiotherapy of cancer. *Adv. Drug Delivery Rev.* **2008**, *60*, 1329–1346.

[10] Zhang, L.; Chen, H.; Wang, L.; Liu, T.; Yeh, J.; Lu, G.; Yang, L.; Mao, H. Delivery of therapeutic radioisotopes using nanoparticle platforms: Potential benefit in systemic radiation therapy. *Nanotechnol. Sci. Appl.* **2010**, *3*, 159–170.

[11] Lim, K.; Stewart, J.; Kelly, V.; Xie, J.; Brock, K. K.; Moseley, J.; Cho, Y.-B.; Fyles, A.; Lundin, A.; Rehbinder, H. et al. Dosimetrically triggered adaptive intensity modulated radiation therapy for cervical cancer. *Int. J. Radiat. Oncol. Biol. Phys.* **2014**, *90*, 147–154.
[12] Macedo, F.; Ladeira, K.; Pinho, F.; Saraiva, N.; Bonito, N.; Pinto, L.; Goncalves, F. Bone metastases: An overview. *Oncol. Rev.* **2017**, *11*, 321.
[13] Wells, S. A., Jr.; Asa, S. L.; Dralle, H.; Elisei, R.; Evans, D. B.; Gagel, R. F.; Lee, N.; Machens, A.; Moley, J. F.; Pacini, F. et al. Revised american thyroid association guidelines for the management of medullary thyroid carcinoma. *Thyroid* **2015**, *25*, 567–610.
[14] Shirato, H.; Le, Q. T.; Kobashi, K.; Prayongrat, A.; Takao, S.; Shimizu, S.; Giaccia, A.; Xing, L.; Umegaki, K. Selection of external beam radiotherapy approaches for precise and accurate cancer treatment. *J. Radiat. Res.* **2018**, *59*, i2–i10.
[15] Barker, H. E.; Paget, J. T.; Khan, A. A.; Harrington, K. J. The tumour microenvironment after radiotherapy: Mechanisms of resistance and recurrence. *Nat. Rev. Cancer* **2015**, *15*, 409–425.
[16] Peng, J.; Yang, Q.; Shi, K.; Xiao, Y.; Wei, X.; Qian, Z. Intratumoral fate of functional nanoparticles in response to microenvironment factor: Implications on cancer diagnosis and therapy. *Adv. Drug Delivery Rev.* **2019**, *143*, 37–67.
[17] Fan, W.; Tang, W.; Lau, J.; Shen, Z.; Xie, J.; Shi, J.; Chen, X. Breaking the depth dependence by nanotechnology-enhanced X-ray-excited deep cancer theranostics. *Adv. Mater.* **2019**, *31*, e1806381.
[18] Rancoule, C.; Magné, N.; Vallard, A.; Guy, J. B.; Rodriguezlafrasse, C.; Deutsch, E.; Chargari, C. Nanoparticles in radiation oncology: From bench-side to bedside. *Cancer Lett.* **2016**, *375*, 256–262.
[19] Song, G. S.; Cheng, L.; Chao, Y.; Yang, K.; Liu, Z. Emerging nanotechnology and advanced materials for cancer radiation therapy. *Adv. Mater.* **2017**, *29*, 1700996.
[20] Haume, K.; Rosa, S.; Grellet, S.; Smialek, M. A.; Butterworth, K. T.; Solov'yov, A. V.; Prise, K. M.; Golding, J.; Mason, N. J. Gold nanoparticles for cancer radiotherapy: A review. *Cancer Nanotechnol.* **2016**, *7*, 8.
[21] Wang, A. Z.; Tepper, J. E. Nanotechnology in radiation oncology. *J. Clin. Oncol.* **2014**, *32*, 2879–2885.
[22] Maeda, H.; Nakamura, H.; Fang, J. The EPR effect for macromolecular drug delivery to solid tumors: Improvement of tumor uptake, lowering of systemic toxicity, and distinct tumor imaging *in vivo*. *Adv. Drug Delivery Rev.* **2013**, *65*, 71–79.
[23] Wardman, P. Chemical radiosensitizers for use in radiotherapy. *Clin. Oncol.* **2007**, *19*, 397–417.
[24] Yang, Y. S.; Carney, R. P.; Stellacci, F.; Irvine, D. J. Enhancing radiotherapy by lipid nanocapsule-mediated delivery of amphiphilic gold nanoparticles to intracellular membranes. *ACS Nano* **2014**, *8*, 8992–9002.
[25] Al Zaki, A.; Joh, D.; Cheng, Z.; De Barros, A. L.; Kao, G.; Dorsey, J.; Tsourkas, A. Gold-loaded polymeric micelles for computed tomography-guided radiation therapy treatment and radiosensitization. *ACS Nano* **2014**, *8*, 104–112.
[26] Cheng, L.; Shen, S.; Shi, S.; Yi, Y.; Liu, Z. $FeSe_2$-decorated Bi_2Se_3 nanosheets fabricated via cation exchange for chelator-free ^{64}Cu-labeling and multimodal image-guided photothermal-radiation therapy. *Adv. Funct. Mater.* **2016**, *26*, 2185–2197.
[27] He, Y.; Chen, W.; Li, X.; Zhang, Z.; Fu, J.; Zhao, C.; Xie, E. Freestanding three-dimensional graphene/MnO_2 composite networks as ultra light and flexible supercapacitor electrodes. *ACS nano* **2013**, *7*, 174–182.
[28] Yermolayeva, Y. V.; Korshikova, T. I.; Tolmachev, A. V.; Yavetskiy, R. P. X-ray luminescence of core-shell structured $SiO_2/Lu_2O_3:Eu^{3+}$ and $SiO_2/Lu_2Si_2O_7:Eu^{3+}$ particles. *Radiat. Meas.* **2011**, *46*, 551–554.
[29] Zhang, X.; Luo, Z.; Jie, C.; Xiu, S.; Xie, J. Ultrasmall Au 10−12 (sg) 10−12 nanomolecules for high tumor specificity and cancer radiotherapy. *Adv. Mater.* **2014**, *26*, 4565–4568.
[30] Zhao, N.; Yan, L.; Zhao, X.; Chen, X.; Li, A.; Zheng, D.; Zhou, X.; Dai, X.; Xu, F. J. Versatile types of organic/inorganic nanohybrids: From strategic design to biomedical applications. *Chem. Rev.* **2019**, *119*, 1666–1762.
[31] Xie, J.; Gong, L.; Zhu, S.; Yong, Y.; Gu, Z.; Zhao, Y. Emerging strategies of nanomaterial-mediated tumor radiosensitization. *Adv. Mater.* **2019**, *31*, e1802244.
[32] Cao, W.; Gu, Y.; Meineck, M.; Xu, H. The combination of chemotherapy and radiotherapy towards more efficient drug delivery. *Chem. – Asian J.* **2014**, *9*, 48–57.
[33] Seiwert, T. Y.; Salama, J. K.; Vokes, E. E. The concurrent chemoradiation paradigm – general principles. *Nat. Clin. Pract. Oncol.* **2007**, *4*, 86–100.
[34] Seiwert, T. Y.; Salama, J. K.; Vokes, E. E. The chemoradiation paradigm in head and neck cancer. *Nat. Clin. Pract. Oncol.* **2007**, *4*, 156–171.
[35] Sun, D.; Chen, J.; Wang, Y.; Ji, H.; Peng, R.; Jin, L.; Wu, W. Advances in refunctionalization of erythrocyte-based nanomedicine for enhancing cancer-targeted drug delivery. *Theranostics* **2019**, *9*, 6885–6900.
[36] Oliveira Pinho, J.; Matias, M.; Gaspar, M. M. Emergent nanotechnological strategies for systemic chemotherapy against melanoma. *Nanomaterials* **2019**, *9*, E1455.
[37] Curran, W. J., Jr.; Paulus, R.; Langer, C. J.; Komaki, R.; Lee, J. S.; Hauser, S.; Movsas, B.; Wasserman, T.; Rosenthal, S. A.; Gore, E. et al. Sequential vs. concurrent chemoradiation for stage III non-small cell lung cancer: Randomized phase III trial RTOG 9410. *J. Natl. Cancer Inst.* **2011**, *103*, 1452–1460.
[38] Lungu, I. I.; Grumezescu, A. M.; Volceanov, A.; Andronescu, E. Nanobiomaterials used in cancer therapy: An up-to-date overview. *Molecules* **2019**, *24*, 3547.
[39] Raza, F.; Zafar, H.; You, X.; Khan, A.; Wu, J.; Ge, L. Cancer nanomedicine: Focus on recent developments and self-assembled peptide nanocarriers. *J. Mater. Chem. B* **2019**, *7*, 7639–7655.
[40] Eloy, J. O.; Petrilli, R.; Trevizan, L. N. F.; Chorilli, M. Immunoliposomes: A review on functionalization strategies and targets for drug delivery. *Colloids Surf., B* **2017**, *159*, 454–467.
[41] Davies, C. d. L.; Lundstrøm, L. M.; Frengen, J.; Eikenes, L.; Bruland S, Ø. S.; Kaalhus, O.; Hjelstuen, M. H. B.; Brekken, C. Radiation improves the distribution and uptake of liposomal doxorubicin (CAELYX) in human osteosarcoma xenografts. *Cancer Res.* **2004**, *64*, 547–553.
[42] Zhang, X.; Yang, H.; Gu, K.; Chen, J.; Rui, M.; Jiang, G.-L. *In vitro* and *in vivo* study of a nanoliposomal cisplatin as a radiosensitizer. *Int. J. Nanomed.* **2011,** *6*, 437–444.
[43] Liu, H.; Xie, Y.; Zhang, Y.; Cai, Y.; Li, B.; Mao, H.; Liu, Y.; Lu, J.; Zhang, L.; Yu, R. Development of a hypoxia-triggered and hypoxic radiosensitized liposome as a doxorubicin carrier to promote synergetic chemo-/radio-therapy for glioma. *Biomaterials* **2017**, *121*, 130–143.
[44] Zhang, R.; Song, X.; Liang, C.; Yi, X.; Song, G.; Chao, Y.; Yang, Y.; Yang, K.; Feng, L.; Liu, Z. Catalase-loaded cisplatin-prodrug-constructed liposomes to overcome tumor hypoxia for enhanced chemo-radiotherapy of cancer. *Biomaterials* **2017**, *138*, 13–21.
[45] Swain, S.; Sahu, P. K.; Beg, S.; Babu, S. M. Nanoparticles for cancer targeting: Current and future directions. *Curr. Drug Delivery* **2016**, *13*, 1290–1302.
[46] Baumann, B. C.; Kao, G. D.; Mahmud, A.; Harada, T.; Swift, J.; Chapman, C.; Xu, X.; Discher, D. E.; Dorsey, J. F. Enhancing the efficacy of drug-loaded nanocarriers against brain tumors by targeted radiation therapy. *Oncotarget* **2013**, *4*, 64–79.
[47] Yu, Y.; Xu, S.; You, H.; Zhang, Y.; Yang, B.; Sun, X.; Yang, L.; Chen, Y.; Fu, S.; Wu, J. *In vivo* synergistic anti-tumor effect of paclitaxel nanoparticles combined with radiotherapy on human cervical carcinoma. *Drug Delivery* **2017**, *24*, 75–82.
[48] Mao, H.; Xie, Y.; Ju, H.; Mao, H.; Zhao, L.; Wang, Z.; Hua, L.; Zhao, C.; Li, Y.; Yu, R. et al. Design of tumor microenvironment-responsive drug-drug micelle for cancer radiochemotherapy. *ACS Appl. Mater. Interfaces* **2018**, *10*, 33923–33935.
[49] Cui, F.-B.; Li, R.-T.; Liu, Q.; Wu, P.-Y.; Hu, W.-J.; Yue, G.-F.; Ding, H.; Yu, L.-X.; Qian, X.-P.; Liu, B.-R. Enhancement of radiotherapy efficacy by docetaxel-loaded gelatinase-stimuli PEG-PEP-PCL nanoparticles in gastric cancer. *Cancer Lett.* **2014**, *346*, 53–62.
[50] Wiedenmann, N.; Valdecanas, D.; Hunter, N.; Hyde, S.; Buchholz, T. A.; Milas, L.; Mason, K. A. 130-nm albumin-bound paclitaxel enhances tumor radiocurability and therapeutic gain. *Clin. Cancer Res.* **2007**, *13*, 1868–1874.
[51] Bouras, A.; Kaluzova, M.; Hadjipanayis, C. G. Radiosensitivity enhancement of radioresistant glioblastoma by epidermal growth

factor receptor antibody-conjugated iron-oxide nanoparticles. *J. Neuro-Oncol.* **2015**, *124*, 13–22.

[52] Meng, L.; Cheng, Y.; Gan, S.; Zhang, Z.; Tong, X.; Xu, L.; Jiang, X.; Zhu, Y.; Wu, J.; Yuan, A. et al. Facile deposition of manganese dioxide to albumin-bound paclitaxel nanoparticles for modulation of hypoxic tumor microenvironment to improve chemoradiation therapy. *Mol. Pharmaceutics* **2018**, *15*, 447–457.

[53] Wang, Z.; Shao, D.; Chang, Z.; Lu, M.; Wang, Y.; Yue, J.; Yang, D.; Li, M.; Xu, Q.; Dong, W.-F. Janus gold nanoplatform for synergetic chemoradiotherapy and computed tomography imaging of hepatocellular carcinoma. *ACS Nano* **2017**, *11*, 12732–12741.

[54] He, L.; Lai, H.; Chen, T. Dual-function nanosystem for synergetic cancer chemo-/radiotherapy through ROS-mediated signaling pathways. *Biomaterials* **2015**, *51*, 30–42.

[55] Chen, Y.; Song, G.; Dong, Z.; Yi, X.; Chao, Y.; Liang, C.; Yang, K.; Cheng, L.; Liu, Z. Drug-loaded mesoporous tantalum oxide nanoparticles for enhanced synergetic chemoradiotherapy with reduced systemic toxicity. *Small* **2017**, *13*, 1602869.

[56] GuhaSarkar, S.; Pathak, K.; Sudhalkar, N.; More, P.; Goda, J. S.; Gota, V.; Banerjee, R. Synergistic locoregional chemoradiotherapy using a composite liposome-in-gel system as an injectable drug depot. *Int. J. Nanomed.* **2016**, *11*, 6435–6448.

[57] Xu, S.; Tang, Y. Y.; Yu, Y. X.; Yun, Q.; Yang, J. P.; Zhang, H.; Peng, Q.; Sun, X.; Yang, L. L.; Fu, S. et al. Novel composite drug delivery system as a novel radio sensitizer for the local treatment of cervical carcinoma. *Drug Delivery* **2017**, *24*, 1139–1147.

[58] Lan, M.; Zhao, S.; Liu, W.; Lee, C. S.; Zhang, W.; Wang, P. Photosensitizers for photodynamic therapy. *Adv. Healthcare Mater.* **2019**, *8*, e1900132.

[59] Clement, S.; Deng, W.; Camilleri, E.; Wilson, B. C.; Goldys, E. M. X-ray induced singlet oxygen generation by nanoparticle-photosensitizer conjugates for photodynamic therapy: Determination of singlet oxygen quantum yield. *Sci. Rep.* **2016**, *6*, 19954.

[60] Wang, G. D.; Nguyen, H. T.; Chen, H.; Cox, P. B.; Wang, L.; Nagata, K.; Hao, Z.; Wang, A.; Li, Z.; Xie, J. X-ray induced photodynamic therapy: A combination of radiotherapy and photodynamic therapy. *Theranostics* **2016**, *6*, 2295–2305.

[61] Abliz, E.; Collins, J. E.; Bell, H.; Tata, D. B. Novel applications of diagnostic X-rays in activating a clinical photodynamic drug: Photofrin ii through X-ray induced visible luminescence from "rare-earth" formulated particles. *J. X-Ray Sci. Technol.* **2011**, *19*, 521–530.

[62] Bulin, A. L.; Truillett, C.; Chouikrat, R.; Lux, F.; Frochot, C.; Amans, D.; Ledoux, G.; Tillement, O.; Perriat, P.; Barberi-Heyob, M. et al. X-ray-induced singlet oxygen activation with nanoscintillator-coupled porphyrins. *J. Phys. Chem. C* **2013**, *117*, 21583–21589.

[63] Chen, H.; Sun, X.; Wang, G. D.; Nagata, K.; Hao, Z.; Wang, A.; Li, Z.; Xie, J.; Shen, B. $LiGa_5O_8$:Cr-based theranostic nanoparticles for imaging-guided X-ray induced photodynamic therapy of deep-seated tumors. *Mater. Horiz.* **2017**, *4*, 1092–1101.

[64] Chen, Z.; Zhao, K.; Bu, W.; Ni, D.; Shi, J. Marriage of scintillator and semiconductor for synchronous radiotherapy and deep photodynamic therapy with diminished oxygen dependence. *Angew. Chem., Int. Ed.* **2014**, *127*, 1770–1774.

[65] Elmenoufy, A. H.; Tang, Y. a.; Hu, J.; Xu, H.; Yang, X. A novel deep photodynamic therapy modality combined with CT imaging established via X-ray stimulated silica-modified lanthanide scintillating nanoparticles. *Chem. Commun.* **2015**, *51*, 12247–12250.

[66] Generalov, R.; Kuan, W. B.; Chen, W.; Kristensen, S.; Juzenas, P. Radiosensitizing effect of zinc oxide and silica nanocomposites on cancer cells. *Colloids Surf. B* **2015**, *129*, 79–86.

[67] Homayoni, H.; Jiang, K.; Zou, X.; Hossu, M.; Rashidi, L. H.; Chen, W. Enhancement of protoporphyrin IX performance in aqueous solutions for photodynamic therapy. *Photodiagn. Photodyn. Ther.* **2015**, *12*, 258–266.

[68] Kascakova, S.; Giuliani, A.; Lacerda, S.; Pallier, A.; Mercere, P.; Toth, E.; Refregiers, M. X-ray-induced radiophotodynamic therapy (RPDT) using lanthanide micelles: Beyond depth limitations. *Nano Res.* **2015**, *8*, 2373–2379.

[69] Kirakci, K.; Kubát, P.; Fejfarová, K.; Martinčík, J.; Nikl, M.; Lang, K. X-ray inducible luminescence and singlet oxygen sensitization by an octahedral molybdenum cluster compound: A new class of nanoscintillators. *Inorg. Chem.* **2016**, *55*, 803–809.

[70] Liang, S.; Li, P. P.; Wen, Y.; Lin, X. H.; Yang, H. H. Low-dose X-ray activation of W(VI)-doped persistent luminescence nanoparticles for deep-tissue photodynamic therapy. *Adv. Funct. Mater.* **2018**, *28*, 1707496.

[71] Liu, Y. F.; Chen, W.; Wang, S. P.; Joly, A. G. Investigation of water-soluble X-ray luminescence nanoparticles for photodynamic activation. *Appl. Phys. Lett.* **2008**, *92*, 043901.

[72] Lu, K.; He, C.; Guo, N.; Chan, C.; Ni, K.; Lan, G.; Tang, H.; Pelizzari, C.; Fu, Y.-X.; Spiotto, M. T. et al. Low-dose X-ray radiotherapy-radiodynamic therapy via nanoscale metal-organic frameworks enhances checkpoint blockade immunotherapy. *Nat. Biomed. Eng.* **2018**, *2*, 600–610.

[73] Ma, L.; Zou, X.; Chen, W. A new X-ray activated nanoparticle photosensitizer for cancer treatment. *J. Biomed. Nanotechnol.* **2014**, *10*, 1501–1508.

[74] Rossi, F.; Bedogni, E.; Bigi, F.; Rimoldi, T.; Cristofolini, L.; Pinelli, S.; Alinovi, R.; Negri, M.; Dhanabalan, S. C.; Attolini, G. et al. Porphyrin conjugated SiC/SiO_x nanowires for X-ray-excited photodynamic therapy. *Sci. Rep.* **2015**, *5*, 7606.

[75] Scaffidi, J. P.; Gregas, M. K.; Lauly, B.; Zhang, Y.; Vo-Dinh, T. Activity of psoralen-functionalized nanoscintillators against cancer cells upon X-ray excitation. *ACS Nano* **2011**, *5*, 4679–4687.

[76] Sharmah, A.; Yao, Z.; Lu, L.; Guo, T. X-ray-induced energy transfer between nanomaterials under X-ray irradiation. *J. Phys. Chem. C* **2016**, *120*, 3054–3060.

[77] Takahashi, J.; Misawa, M. Analysis of potential radiosensitizing materials for X-ray-induced photodynamic therapy. *Nanobiotechnology* **2007**, *3*, 116–126.

[78] Tang, Y. a.; Hu, J.; Elmenoufy, A. H.; Yang, X. Highly efficient fret system capable of deep photodynamic therapy established on X-ray excited mesoporous LaF_3:Tb scintillating nanoparticles. *ACS Appl. Mater. Interfaces* **2015**, *7*, 12261–12269.

[79] Wang, Z.; Chiu, Y.-H.; Honz, K.; Mak, K. F.; Shan, J. Electrical tuning of interlayer exciton gases in WSe_2 bilayers. *Nano Lett.* **2018**, *18*, 137–143.

[80] Chen, W.; Zhang, J. Using nanoparticles to enable simultaneous radiation and photodynamic therapies for cancer treatment. *J. Nanosci. Nanotechnol.* **2006**, *6*, 1159–1166.

[81] Abrahamse, H.; Kruger, C. A.; Kadanyo, S.; Mishra, A. Nanoparticles for advanced photodynamic therapy of cancer. *Photomed. Laser Surg.* **2017**, *35*, 581–588.

[82] Yang, M.; Yang, T.; Mao, C. Enhancement of photodynamic cancer therapy by physical and chemical factors. *Angew. Chem., Int. Ed.* **2019**, *58*, 14066–14080.

[83] Zou, X.; Yao, M.; Ma, L.; Hossu, M.; Han, X.; Juzenas, P.; Chen, W. X-ray-induced nanoparticle-based photodynamic therapy of cancer. *Nanomedicine* **2014**, *9*, 2339–2351.

[84] Chen, H.; Wang, G. D.; Chuang, Y.-J.; Zhen, Z.; Chen, X.; Biddinger, P.; Hao, Z.; Liu, F.; Shen, B.; Pan, Z. et al. Nanoscintillator-mediated X-ray inducible photodynamic therapy for *in vivo* cancer treatment. *Nano Lett.* **2015**, *15*, 2249–2256.

[85] Ahmad, F.; Wang, X.; Jiang, Z.; Yu, X.; Liu, X.; Mao, R.; Chen, X.; Li, W. Codoping enhanced radioluminescence of nanoscintillators for X-ray-activated synergistic cancer therapy and prognosis using metabolomics. *ACS Nano* **2019**, *13*, 10419–10433.

[86] Zhong, X.; Wang, X.; Zhan, G.; Tang, Y. a.; Yao, Y.; Dong, Z.; Hou, L.; Zhao, H.; Zeng, S.; Hu, J. et al. $NaCeF_4$:Gd,Tb scintillator as an X-ray responsive photosensitizer for multimodal imaging-guided synchronous radio/radiodynamic therapy. *Nano Lett.* **2019**, *19*, 8234–8244.

[87] Ma, L.; Zou, X.; Bui, B.; Chen, W.; Song, K. H.; Solberg, T. X-ray excited ZnS:Cu,Co afterglow nanoparticles for photodynamic activation. *Appl. Phys. Lett.* **2014**, *105*, 013702.

[88] Sun, W.; Luo, L.; Feng, Y.; Cai, Y.; Zhuang, Y.; Xie, R.-J.; Chen, X.; Chen, H. Aggregation-induced emission gold clustoluminogens for enhanced low-dose X-ray-induced photodynamic therapy. *Angew. Chem., Int. Ed.* **2019**, *58*, 1–8..

[89] Sun, W.; Shi, T.; Luo, L.; Chen, X.; Lv, P.; Lv, Y.; Zhuang, Y.; Zhu, J.; Liu, G.; Chen, X. et al. Monodisperse and uniform mesoporous silicate nanosensitizers achieve low-dose X-ray-induced deep-penetrating photodynamic therapy. *Adv. Mater.* **2019**, *31*, e1808024.

[90] Lan, G.; Ni, K.; Xu, R.; Lu, K.; Lin, Z.; Chan, C.; Lin, W. Nanoscale

metal-organic layers for deeply penetrating X-ray-induced photodynamic therapy. *Angew. Chem., Int. Ed.* **2017**, *56*, 12102–12106.

[91] Ni, K.; Lan, G.; Veroneau, S. S.; Duan, X.; Song, Y.; Lin, W. Nanoscale metal-organic frameworks for mitochondria-targeted radiotherapy-radiodynamic therapy. *Nat. Commun.* **2018**, *9*, 4321–4321.

[92] Zhang, H.; Cui, W.; Qu, X.; Wu, H.; Qu, L.; Zhang, X.; Mäkilä, E.; Salonen, J.; Zhu, Y.; Yang, Z. et al. Photothermal-responsive nanosized hybrid polymersome as versatile therapeutics codelivery nanovehicle for effective tumor suppression. *Proc. Natl. Acad. Sci. U. S. A.* **2019**, *116*, 7744–7749.

[93] Doughty, A. C. V.; Hoover, A. R.; Layton, E.; Murray, C. K.; Howard, E. W.; Chen, W. R. Nanomaterial applications in photothermal therapy for cancer. *Materials* **2019**, *12*, 779.

[94] Alves, C. G.; Lima-Sousa, R.; de Melo-Diogo, D.; Louro, R. O.; Correia, I. J. Ir780 based nanomaterials for cancer imaging and photothermal, photodynamic and combinatorial therapies. *Int. J. Pharm.* **2018**, *542*, 164–175.

[95] Chen, H.; Zhao, Y. Applications of light-responsive systems for cancer theranostics. *ACS Appl. Mater. Interfaces* **2018**, *10*, 21021–21034.

[96] Lu, S.; Li, X.; Zhang, J.; Peng, C.; Shen, M.; Shi, X. Dendrimer-stabilized gold nanoflowers embedded with ultrasmall iron oxide nanoparticles for multimode imaging-guided combination therapy of tumors. *Adv. Sci.* **2018**, *5*, 1801612.

[97] Wang, S.; You, Q.; Wang, J.; Song, Y.; Cheng, Y.; Wang, Y.; Yang, S.; Yang, L.; Li, P.; Lu, Q. et al. MSOT/CT/MR imaging-guided and hypoxia-maneuvered oxygen self-supply radiotherapy based on one-pot MnO_2-$MSiO_2$@Au nanoparticles. *Nanoscale* **2019**, *11*, 6270–6284.

[98] Deng, Y.; Tian, X.; Lu, S.; Xie, M.; Hu, H.; Zhang, R.; Lv, F.; Cheng, L.; Gu, H.; Zhao, Y. et al. Fabrication of multifoliate PtRu bimetallic nanocomplexes for computed tomography imaging and enhanced synergistic thermoradiotherapy. *ACS Appl. Mater. Interfaces* **2018**, *10*, 31106–31113.

[99] Feng, L.; Dong, Z.; Liang, C.; Chen, M.; Tao, D.; Cheng, L.; Yang, K.; Liu, Z. Iridium nanocrystals encapsulated liposomes as near-infrared light controllable nanozymes for enhanced cancer radiotherapy. *Biomaterials* **2018**, *181*, 81–91.

[100] Li, J.; Zu, X.; Liang, G.; Zhang, K.; Liu, Y.; Li, K.; Luo, Z.; Cai, K. Octopod PtCu nanoframe for dual-modal imaging-guided synergistic photothermal radiotherapy. *Theranostics* **2018**, *8*, 1042–1058.

[101] Tang, W.; Dong, Z.; Zhang, R.; Yi, X.; Yang, K.; Jin, M.; Yuan, C.; Xiao, Z.; Liu, Z.; Cheng, L. Multifunctional two-dimensional core-shell mxene@gold nanocomposites for enhanced photo-radio combined therapy in the second biological window. *ACS nano* **2019**, *13*, 284–294.

[102] Yang, G.; Zhang, R.; Liang, C.; Zhao, H.; Yi, X.; Shen, S.; Yang, K.; Cheng, L.; Liu, Z. Manganese dioxide coated WS_2@Fe_3O_4/$sSiO_2$ nanocomposites for pH-responsive MR imaging and oxygen-elevated synergetic therapy. *Small* **2018**, *14*, 1702664.

[103] Yong, Y.; Cheng, X.; Bao, T.; Zu, M.; Yan, L.; Yin, W.; Ge, C.; Wang, D.; Gu, Z.; Zhao, Y. Tungsten sulfide quantum dots as multifunctional nanotheranostics for *in vivo* dual-modal image-guided photothermal/radiotherapy synergistic therapy. *ACS Nano* **2015**, *9*, 12451–12463.

[104] Li, A.; Li, X.; Yu, X.; Li, W.; Zhao, R.; An, X.; Cui, D.; Chen, X.; Li, W. Synergistic thermoradiotherapy based on PEGylated Cu_3BiS_3 ternary semiconductor nanorods with strong absorption in the second near-infrared window. *Biomaterials* **2017**, *112*, 164–175.

[105] Song, G.; Liang, C.; Gong, H.; Li, M.; Zheng, X.; Cheng, L.; Yang, K.; Jiang, X.; Liu, Z. Core-shell MnSe@Bi_2Se_3 fabricated via a cation exchange method as novel nanotheranostics for multimodal imaging and synergistic thermoradiotherapy. *Adv. Mater.* **2015**, *27*, 6110–6117.

[106] Du, J.; Gu, Z.; Yan, L.; Yong, Y.; Yi, X.; Zhang, X.; Liu, J.; Wu, R.; Ge, C.; Chen, C. et al. Poly(vinylpyrollidone)- and selenocysteine-modified Bi_2Se_3 nanoparticles enhance radiotherapy efficacy in tumors and promote radioprotection in normal tissues. *Adv. Mater.* **2017**, *29*, 1701268.

[107] Wang, J.; Tan, X.; Pang, X.; Liu, L.; Tan, F.; Li, N. MoS_2 quantum dot@polyaniline inorganic-organic nanohybrids for *in vivo* dual-modal imaging guided synergistic photothermal/radiation therapy. *ACS Appl. Mater. Interfaces* **2016**, *8*, 24331–24338.

[108] Xiao, Q.; Zheng, X.; Bu, W.; Ge, W.; Zhang, S.; Chen, F.; Xing, H.; Ren, Q.; Fan, W.; Zhao, K. et al. A core/satellite multifunctional nanotheranostic for *in vivo* imaging and tumor eradication by radiation/photothermal synergistic therapy. *J. Am. Chem. Soc.* **2013**, *135*, 13041–13048.

[109] Zhou, R.; Wang, H.; Yang, Y.; Zhang, C.; Dong, X.; Du, J.; Yan, L.; Zhang, G.; Gu, Z.; Zhao, Y. Tumor microenvironment-manipulated radiocatalytic sensitizer based on bismuth heteropolytungstate for radiotherapy enhancement. *Biomaterials* **2019**, *189*, 11–22.

[110] Zhou, Y.; Hu, Y.; Sun, W.; Lu, S.; Cai, C.; Peng, C.; Yu, J.; Popovtzer, R.; Shen, M.; Shi, X. Radiotherapy-sensitized tumor photothermal ablation using γ-polyglutamic acid nanogels loaded with polypyrrole. *Biomacromolecules* **2018**, *19*, 2034–2042.

[111] Yu, L.; Hu, P.; Chen, Y. Gas-generating nanoplatforms: Material chemistry, multifunctionality, and gas therapy. *Adv. Mater.* **2018**, *30*, e1801964.

[112] Fan, W.; Lu, N.; Shen, Z.; Tang, W.; Shen, B.; Cui, Z.; Shan, L.; Yang, Z.; Wang, Z.; Jacobson, O. et al. Generic synthesis of small-sized hollow mesoporous organosilica nanoparticles for oxygen-independent X-ray-activated synergistic therapy. *Nat. Commun.* **2019**, *10*, 1241.

[113] Liu, J.; Dong, J.; Zhang, T.; Peng, Q. Graphene-based nanomaterials and their potentials in advanced drug delivery and cancer therapy. *J. Control. Release* **2018**, *286*, 64–73.

[114] Fan, W.; Bu, W.; Zhang, Z.; Shen, B.; Zhang, H.; He, Q.; Ni, D.; Cui, Z.; Zhao, K.; Bu, J. et al. X-ray radiation-controlled no-release for on-demand depth-independent hypoxic radiosensitization. *Angew. Chem., Int. Ed.* **2015**, *54*, 14026–14030.

[115] Du, Z.; Zhang, X.; Guo, Z.; Xie, J.; Dong, X.; Zhu, S.; Du, J.; Gu, Z.; Zhao, Y. X-ray-controlled generation of peroxynitrite based on nanosized $LiLuF_4:Ce^{3+}$ scintillators and their applications for radiosensitization. *Adv. Mater.* **2018**, *30*, e1804046.

[116] Gao, M.; Liang, C.; Song, X.; Chen, Q.; Jin, Q.; Wang, C.; Liu, Z. Erythrocyte-membrane-enveloped perfluorocarbon as nanoscale artificial red blood cells to relieve tumor hypoxia and enhance cancer radiotherapy. *Adv. Mater.* **2017**, *29*, 1701429.

[117] Song, G.; Chen, Y.; Liang, C.; Yi, X.; Liu, J.; Sun, X.; Shen, S.; Yang, K.; Liu, Z. Catalase-loaded TaO_x nanoshells as bio-nanoreactors combining high-Z element and enzyme delivery for enhancing radiotherapy. *Adv. Mater.* **2016**, *28*, 7143–7148.

[118] Singh, B. N.; Prateeksha; Gupta, V. K.; Chen, J.; Atanasov, A. G. Organic nanoparticle-based combinatory approaches for gene therapy. *Trends Biotechnol.* **2017**, S0167779917301907.

[119] Xin, Y.; Huang, M.; Guo, W. W.; Huang, Q.; Zhang, L. Z.; Jiang, G. Nano-based delivery of RNAi in cancer therapy. *Mol. Cancer* **2017**, *16*, 134.

[120] Zhou, Z.; Liu, X.; Zhu, D.; Wang, Y.; Zhang, Z.; Zhou, X.; Qiu, N.; Chen, X.; Shen, Y. Nonviral cancer gene therapy: Delivery cascade and vector nanoproperty integration. *Adv. Drug Delivery Rev.* **2017**, *115*, 115–154.

[121] Gaca, S.; Reichert, S.; Multhoff, G.; Wacker, M.; Hehlgans, S.; Botzler, C.; Gehrmann, M.; Rödel, C.; Kreuter, J.; Rödel, F. Targeting by CMHSP70.1-antibody coated and survivin miRNA plasmid loaded nanoparticles to radiosensitize glioblastoma cells. *J. Control. Release* **2013**, *172*, 201–206.

[122] Yong, Y.; Zhang, C.; Gu, Z.; Du, J.; Guo, Z.; Dong, X.; Xie, J.; Zhang, G.; Liu, X.; Zhao, Y. Polyoxometalate-based radiosensitization platform for treating hypoxic tumors by attenuating radioresistance and enhancing radiation response. *ACS Nano* **2017**, *11*, 7164–7176.

[123] Riley, R. S.; June, C. H.; Langer, R.; Mitchell, M. J. Delivery technologies for cancer immunotherapy. *Nat. Rev. Drug Discovery* **2019**, *18*, 175–196.

[124] Huang, S.; Zhao, Q. Nanomedicine-combined immunotherapy for cancer. *Curr. Med. Chem.* **2019**, *26*, 1–14.

[125] Carvalho, H. d. A.; Villar, R. C. Radiotherapy and immune response: The systemic effects of a local treatment. *Clinics* **2018**, *73*, e557s.

[126] Filatenkov, A.; Baker, J.; Mueller, A. M. S.; Kenkel, J.; Ahn, G. O.; Dutt, S.; Zhang, N.; Kohrt, H.; Jensen, K.; Dejbakhsh-Jones, S. et al. Ablative tumor radiation can change the tumor immune cell

microenvironment to induce durable complete remissions. *Clin. Cancer Res.* **2015**, *21*, 3727–3739.

[127] McBride, W. H.; Chiang, C.-S.; Olson, J. L.; Wang, C.-C.; Hong, J.-H.; Pajonk, F.; Dougherty, G. J.; Iwamoto, K. S.; Pervan, M.; Liao, Y.-P. A sense of danger from radiation. *Radiat. Res.* **2004,** *162*, 1–19.

[128] Schaue, D.; Kachikwu, E. L.; McBride, W. H. Cytokines in radiobiological responses: A review. *Radiat. Res.* **2012**, *178*, 505–523.

[129] Weichselbaum, R. R.; Liang, H.; Deng, L.; Fu, Y.-X. Radiotherapy and immunotherapy: A beneficial liaison? *Nat. Rev. Clin. Oncol.* **2017**, *14*, 365–379.

[130] Sharabi, A. B.; Lim, M.; DeWeese, T. L.; Drake, C. G. Radiation and checkpoint blockade immunotherapy: Radiosensitisation and potential mechanisms of synergy. *Lancet Oncol.* **2015**, *16*, e498–e509.

[131] Song, W.; Musetti, S. N.; Huang, L. Nanomaterials for cancer immunotherapy. *Biomaterials* **2017**, *148*, 16–30.

[132] Zhang, P.; Zhai, Y.; Cai, Y.; Zhao, Y.; Li, Y. Nanomedicine-based immunotherapy for the treatment of cancer metastasis. *Adv. Mater.* **2019**, e1904156.

[133] Kubackova, J.; Zbytovska, J.; Holas, O. Nanomaterials for direct and indirect immunomodulation: A review of applications. *Eur. J. Pharm. Sci.* **2019**, 105139.

[134] Wang, C.; Fan, W.; Zhang, Z.; Wen, Y.; Xiong, L.; Chen, X. Advanced nanotechnology leading the way to multimodal imaging-guided precision surgical therapy. *Adv. Mater.* **2019**, e1904329.

[135] Min, Y.; Roche, K. C.; Tian, S.; Eblan, M. J.; McKinnon, K. P.; Caster, J. M.; Chai, S.; Herring, L. E.; Zhang, L.; Zhang, T. et al. Antigen-capturing nanoparticles improve the abscopal effect and cancer immunotherapy. *Nat. Nanotechnol.* **2017**, *12*, 877–882.

[136] Appelbe, O. K.; Moynihan, K. D.; Flor, A.; Rymut, N.; Irvine, D. J.; Kron, S. J. Radiation-enhanced delivery of systemically administered amphiphilic-CPG oligodeoxynucleotide. *J. Control. Release* **2017**, *266*, 248–255.

[137] Au, K. M.; Balhorn, R.; Balhorn, M. C.; Park, S. I.; Wang, A. Z. High-performance concurrent chemo-immuno-radiotherapy for the treatment of hematologic cancer through selective high-affinity ligand antibody mimic-functionalized doxorubicin-encapsulated nanoparticles. *ACS Cent. Sci.* **2019**, *5*, 122–144.

[138] Meng, L.; Cheng, Y.; Tong, X.; Gan, S.; Ding, Y.; Zhang, Y.; Wang, C.; Xu, L.; Zhu, Y.; Wu, J. et al. Tumor oxygenation and hypoxia inducible factor-1 functional inhibition via a reactive oxygen species responsive nanoplatform for enhancing radiation therapy and abscopal effects. *ACS Nano* **2018**, *12*, 8308–8322.

[139] Chen, Q.; Chen, J.; Yang, Z.; Xu, J.; Xu, L.; Liang, C.; Han, X.; Liu, Z. Nanoparticle-enhanced radiotherapy to trigger robust cancer immunotherapy. *Adv. Mater.* **2019**, *31*, e1802228.

[140] Guo, Z.; Zhu, S.; Yong, Y.; Zhang, X.; Dong, X.; Du, J.; Xie, J.; Wang, Q.; Gu, Z.; Zhao, Y. Synthesis of BSA-coated BiOI@Bi_2S_3 semiconductor heterojunction nanoparticles and their applications for radio/photodynamic/photothermal synergistic therapy of tumor. *Adv. Mater.* **2017**, *29*, 1704136.

[141] Huang, P.; Zhang, Y.; Wang, W.; Zhou, J.; Sun, Y.; Liu, J.; Kong, D.; Liu, J.; Dong, A. Co-delivery of doxorubicin and ^{131}I by thermosensitive micellar-hydrogel for enhanced *in situ* synergetic chemoradiotherapy. *J. Control. Release* **2015**, *220*, 456–464.

[142] Shih, Y.-H.; Peng, C.-L.; Chiang, P.-F.; Lin, W.-J.; Luo, T.-Y.; Shieh, M.-J. Therapeutic and scintigraphic applications of polymeric micelles: Combination of chemotherapy and radiotherapy in hepatocellular carcinoma. *Int. J. Nanomed.* **2015**, *10*, 7443–7454.

[143] Werner, M. E.; Karve, S.; Sukumar, R.; Cummings, N. D.; Copp, J. A.; Chen, R. C.; Zhang, T.; Wang, A. Z. Folate-targeted nanoparticle delivery of chemo- and radiotherapeutics for the treatment of ovarian cancer peritoneal metastasis. *Biomaterials* **2011**, *32*, 8548–8554.

[144] Zhou, M.; Chen, Y.; Adachi, M.; Wen, X.; Erwin, B.; Mawlawi, O.; Lai, S. Y.; Li, C. Single agent nanoparticle for radiotherapy and radio-photothermal therapy in anaplastic thyroid cancer. *Biomaterials* **2015**, *57*, 41–49.

[145] Chen, L.; Zhong, X.; Yi, X.; Huang, M.; Ning, P.; Liu, T.; Ge, C.; Chai, Z.; Liu, Z.; Yang, K. Radionuclide ^{131}I labeled reduced graphene oxide for nuclear imaging guided combined radio- and photothermal therapy of cancer. *Biomaterials* **2015**, *66*, 21–28.

[146] Meng, Z.; Chao, Y.; Zhou, X.; Liang, C.; Liu, J.; Zhang, R.; Cheng, L.; Yang, K.; Pan, W.; Zhu, M. et al. Near-infrared-triggered *in situ* gelation system for repeatedly enhanced photothermal brachytherapy with a single dose. *ACS Nano* **2018**, *12*, 9412–9422.

[147] Tian, L.; Chen, Q.; Yi, X.; Chen, J.; Liang, C.; Chao, Y.; Yang, K.; Liu, Z. Albumin-templated manganese dioxide nanoparticles for enhanced radioisotope therapy. *Small* **2017**, *13*, 1700640.